PMFSEL REPORT NO. 96-1

THE EFFECT OF END DISTANCE ON THE BEARING STRENGTH OF BOLTED CONNECTIONS

by

HYEONG JUN KIM and JOSEPH A YURA

February, 1996

THE EFFECT OF END DISTANCE
ON THE BEARING STRENGTH OF BOLTED CONNECTIONS

by

Hyeong Jun Kim, B.S.

Thesis

Presented to the Faculty of the Graduate School

of The University of Texas at Austin

in Partial Fulfillment

of the Requirements

for the Degree of

Master of Science in Engineering

The University of Texas at Austin

May, 1996

THE EFFECT OF END DISTANCE

ON THE BEARING STRENGTH OF BOLTED CONNECTIONS

APPROVED BY

SUPERVISING COMMITTEE:

_____

_____

ACKNOWLEDGMENTS

I would like to thank Dr. Joseph A. Yura for his guidance and advice from the beginning to the end of this work. Especially for the preparation of the experiment, his help was more than anyone could give. I would also like to express my gratitude to Dr. Karl H. Frank for his knowledge and advice on this work. Special thanks goes to the permanent staff of the Phil M. Ferguson Laboratory. This work would have been much harder without their support and assistance.

This work was conducted with the supply of the high strength steel plates from the Butler Manufacturing Company. Their kind assistance is gratefully acknowledged.

Finally, I would like to thank my parents and Sarah for their love and support.

Hyeong Jun Kim

The University of Texas at Austin
February, 1996

ABSTRACT

THE EFFECT OF END DISTANCE

ON THE BEARING STRENGTH OF BOLTED CONNECTIONS

by

Hyeong Jun Kim, M.S.E.

The University of Texas at Austin, 1996

SUPERVISOR: Joseph A. Yura

An experimental study on the effect of end distance on the bearing strength of bolted connections was undertaken. Single bolt and two-bolt lap splices were used in the study. Two different steels were used in the test program to determine the effect of steel strength on the end distance strength. One steel had high ultimate stress to yield stress ratio and the other steel had low ultimate stress to yield stress ratio. Experiments on lap splices with various clear end distances and clear spacings were carried out. It was determined that ultimate stress to yield stress ratio does not affect the strength at 1/4 in. displacement, and it is reconfirmed that the bearing strength is proportional to the ultimate stress. The results are compared with the strength predicted by the AISC-LRFD design equations and by a clear distance approach.

TABLE OF CONTENTS

Chapter One: Introduction 1

General 1

Previous Research 5

Objectives and Scope 8

Chapter Two: Test Program 10

Test Variables 10

Specimen 10

Test Setup 17

Measurements 17

Test Setup Modifications 18

Test Procedure 23

Calculations 24

Problems Associated with the Measurement 25

Notation 26

Chapter Three: Test Results 27

Results 27

Observations 34

Failure Mode 54

Chapter Four: Comparison with Desgin Equations 57

Comparison with AISC-LRFD and Design Equations in Reference 12..... 57

Comparison with Other Strength Predictions 58

Chapter Five: Conclusions 68

Appendix 69

List of References 83

LIST OF TABLES

Table 2-1 Material Properties 15
Table 3-1 Test Results 29
Table 3-2 Effect of Short End Distance(AT Series) 52
Table 3-3 Effect of Short End Distance(BT Series) 52
Table A 69

LIST OF FIGURES

Figure 1-1 Theoretical Model 2
Figure 1-2 Dimensions 2
Figure 1-3 Comparison of Design Equations with Test Results[From Reference 8] 3
Figure 2-1 Preparation of the Test Specimen 13
Figure 2-2 Diameter of the Punched Hole 13
Figure 2-3 Specimen for AW Test Series 14
Figure 2-4 Specimen for AO and BO Test Series 14
Figure 2-5 Specimen for AT and BT Test Series 14
Figure 2-6 Coupon Test Results 16
Figure 2-7 Test Setup 19
Figure 2-8 Displacement Measurement 21
Figure 2-9 The Clamping Device: Modification 1 21
Figure 2-10 The Clamping Device: Modification 2..... 22
Figure 2-11 Initial Crookedness and Lateral Force 22
Figure 2-12 Displacement Measurement 2 23
Figure 2-13 Elastic Deformation 24
Figure 2-14 Rotation of the Clamping Device 25
Figure 3-1 Plot of Modified Displacement and Load Data(BO200) 28
Figure 3-2 Effect of Width on One-bolt Specimen 30
Figure 3-3 End Buckling 31
Figure 3-4 Effect of Lateral Confinement 33
Figure 3-5 Strength Normalized by Yield Stress(1/4 in. Disp.) 35
Figure 3-6 Strength Normalized by Yield Stress(at Ultimate) 36
Figure 3-7 Strength Normalized by Ultimate Stress(1/4 in. Disp.) 37
Figure 3-8 Strength Normalized by Ultimate Stress(at Ultimate) 38
Figure 3-9 Comparison of Ductility 42
Figure 3-10 Effect of End Distance on Deformation Capacity 43
Figure 3-11 Deformation Capacity 44

Figure 3-12 Load-Displacement Curve of Specimen BO150 46
Figure 3-13 Critical Section 54
Figure 3-14 Yield Lines 54
Figure 3-15 Fracture 55
Figure 3-16 Yielding at the Edge of a Specimen 56
Figure 4-1 Comparison of Test Results with AISC-LRFD(1/4 in. Disp.) 60
Figure 4-2 Comparison of Test Results with AISC-LRFD(at Ultimate) 61
Figure 4-3 Comparison of Test Results with Clear Distance Appoach(1/4 in. Disp.) ... 62
Figure 4-4 Comparison of Test Results with Clear Distance Approach(at Ultimate) ... 63
Figure 4-5 Comparison of Test Results with AISC-LRFD(Spacing > 3.0d) 64
Figure 4-6 Comparison with Design Equations(Ref. 8) 65
Figure 4-7 Comparison with Design Equations(Ref. 11, 3, 7) 66
Figure 4-8 Comparison of the Test Results by Lewis[9] with AISC-LRFD 67
Figure A 69
Figure B-1-1 AW300 71
Figure B-1-2 AW350 and AW35R 71
Figure B-1-3 AW45S and AW45U 72
Figure B-1-4 AW600 72
Figure B-2-1 AO050 and AO050R 73
Figure B-2-2 AO100 73
Figure B-2-3 AO150 74
Figure B-3-1 AT0510 and AT0510R 75
Figure B-3-2 AT0520 and AT0520R 75
Figure B-3-3 AT0530 and AT0530R 76
Figure B-3-4 AT1510 and AT1510R 76
Figure B-3-5 AT1520 and AT1520R 77
Figure B-3-6 AT1530 and AT1530R 77
Figure B-4-1 BO050 and BO050R 78
Figure B-4-2 BO100 and BO100R 78

Figure B-4-3 BO150 and BO150R 79
Figure B-4-4 BO200 and BO200R 79
Figure B-5-1 BT0510 and BT0510R 80
Figure B-5-2 BT0520 and BT0520R 80
Figure B-5-3 BT0530 and BT0530R 81
Figure B-5-4 BT1510 and BT1510R 81
Figure B-5-5 BT1520 and BT1520R 82
Figure B-5-6 BT1530 and BT1530R 82

LIST OF PHOTOS

Photo 1 Test Setup 20
Photo 2 Failure of Specimen AW350 40
Photo 3 Failure of Specimen AO050 40
Photo 4 Failure of Specimen AO100 41
Photo 5 Buckling at Free End of Specimen AO200R 41
Photo 6 Initial Stage 47
Photo 7 Yielding around Hole 47
Photo 8 Yield Lines 47
Photo 9 Thickening of Yield Lines 47
Photo 10 Complete Yielding 47
Photo 11 Fracture at the End 47
Photo 12 Stress Concentration on the Top Edge of the First Bolt Hole 49
Photo 13 Fracture due to Tensile Stress 49
Photo 14 Tensile Fracture at the Top Edge of the First Bolt Hole 50
Photo 15 Fracture at the End 50
Photo 16 Yield Lines between Bolt Holes 53
Photo 17 Bending of Bolt 53

NOMENCLATURE

C1	- clear end distance
C2	- clear spacing
d	- diameter of the bolt
d_h	- diameter of the hole
F_b	- bearing stress
F_u	- ultimate stress of the connected material
F_y	- yield stress of the connected material
L_e	- end distance
$P_{1/4}$	- bearing strength at 1/4 in. hole elongation
P_u	- bearing strength at ultimate
$P_{1/4, Clear}$	- bearing strength at 1/4 in. hole elongation predicted by a clear distance approach
$P_{u, Clear}$	- bearing strength at ultimate predicted by a clear distance approach.
$P_{1/4, LRFD}$	- bearing strength at 1/4 in. hole elongation predicted by AISC-LRFD
$P_{u, LRFD}$	- bearing strength at ultimate predicted by AISC-LRFD
R_n	- nominal bearing strength
s	- spacing
t	- thickness of the connected plate
w	- width of the connected plate

CHAPTER 1

Introduction

1.1 General

When a bolt bears on the edge of the hole in a bolted shear connection, the stress concentration near the bolt hole has a significant effect on the strength of the connection. The stress concentration causes localized yielding or fracture around the hole, which leads to the failure of the connection[8].* The strength of the connection which is governed by this stress distribution is estimated by two types of equations, one is for the bearing failure mode and the other is for the end tearout failure mode. End distance and spacing of the holes have a major influence on the shape of the stress distribution in the connection. Therefore, end distance and spacings are used as measures to determine whether the failure mode would be a bearing failure or an end tearout failure.

Currently, the strength of bearing-type connections is considered to be proportional to end distance and spacing based on hole centerline dimensions. They have been used for estimating the strength for a long time even though a theoretical model using the clear distances seems to be more logical measure of determining the strength[8, 12]. The theoretical model dealing with the end tearout failure mode is shown in Figure 1-1. The solid lines are actual failure lines and the horizontal dashed lines are lower bound failure lines where a transmitted force is assumed to be resisted by the shear force developed along the lines. If the shear strength of a steel is considered to be 70% of the tensile strength[Kulak *et al*(1987)], then, the shear resistance along the dashed lines is estimated as $R_n = 2t(C1)(0.7F_u)$, that is, $1.4(C1)tF_u$. As shown in Figure 1-2, the clear distance is defined as the distance along the line of force from the edge of the hole to the end of the connected member for clear end distance, and to the edge of the adjacent hole for clear spacing. Conventional end distance and spacing are measured from the center of the hole to the end of the connected member, and to the center of the adjacent hole respectively. For the connections with standard holes, the clear end

* References are listed out the end of Appendix

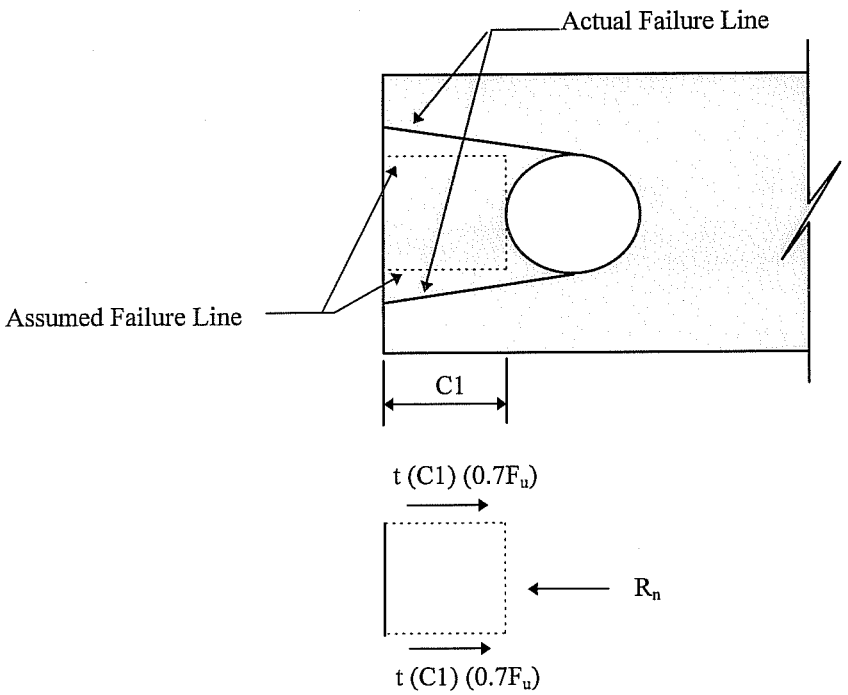

Figure 1-1 Theoretical Model

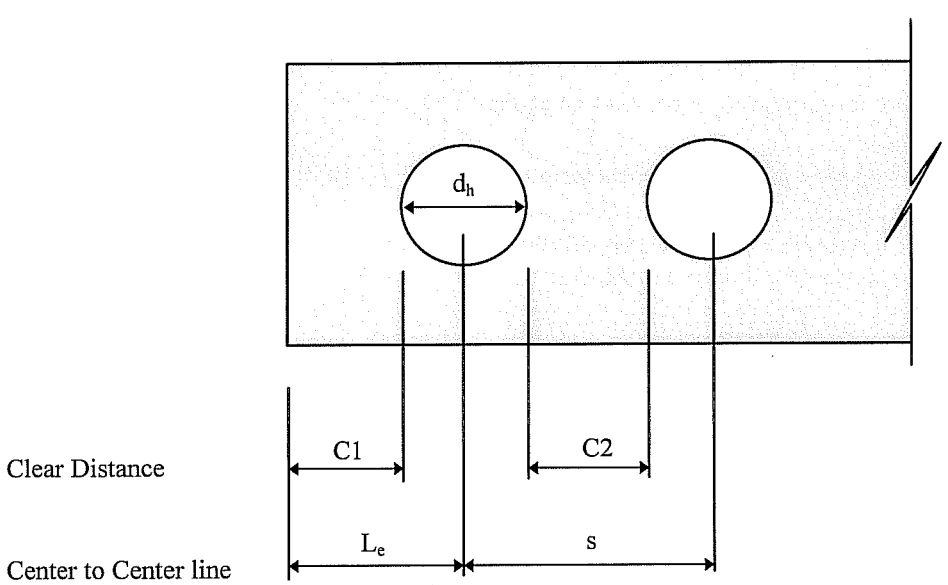

Figure 1-2 Dimensions

distance is smaller than the end distance by half of the diameter of the hole. Since C1 is L_e-$d_h/2$, the shear resistance can be expressed as $R_n = 1.4(L_e-d_h/2)tF_u$. Dividing both sides of the equation by d_ht results in $R_n/(d_ht) = 1.4(L_e/d_h-0.5)F_u$. If $R_n/(d_ht)$ is replaced with the bearing stress, F_b, and if the the equation is rearranged, it becomes $L_e/d_h = 0.5 +0.715(F_b/F_u)$. If the L_e/d_h ratio is within the range of 1.0 to 3.0, this equation can be approximated by the equation $L_e/d_h = F_b/F_u$. This alternative equation results in the the estimation of the shear resistance in terms of the centerline dimension instead of the clear dimensions. Replacing F_b with $R_n/(d_ht)$, and rearranging the alternative equation, the shear resistance is estimated as $R_n = L_etF_u$. Both $1.4(C1)tF_u$ and L_etF_u are in good agreement with the test results as shown in Figure 1-3. In Reference 12, the shear strength is assumed to be 60% of the tensile strength, which results in the shear resistance of $1.2(C1)t\ F_u$. These equations only deal with the end tearout failure mode. As the L_e/d_h ratio gets high, the failure mode gradually changes from the end tearout to the bearing. Separate equations are used for the bearing failure mode.

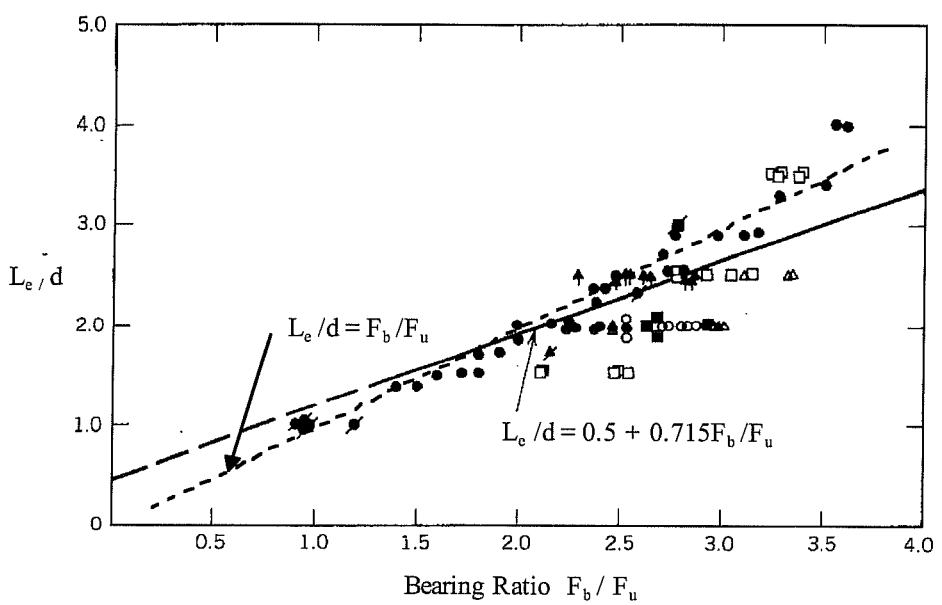

Figure 1-3 Comparison of Design Equations with Test Results[From Reference 8]

As the load which is transmitted through the connection increases, material around the hole yields and fractures. Before fracture occurs, the connected plates move relative to each other because of the deformation around the hole. The hole deformation can change the overall configuration of the connection and the structure. Currently, 1/4 in. hole elongation is used as one of the limit conditions when the change of configuration can significantly affect the overall strength and usefulness of the structure.

The ultimate stress of the connected member is considered to be a representative material property where the failure is due to fracture. But, the fracture may or may not occur at 1/4 in. hole elongation. Significant displacement is usually associated with the yielding of the material. Therefore, the yield stress of the connected material rather than the ultimate stress may have a governing effect on the strength at 1/4 in. displacement. This leads to a possibility that a high strength steel which has low ultimate to yield stress ratio may have different behavior from a steel which has high ultimate to yield stress ratio. Signficant yielding around the hole would occur before the fracture occurs for a connections with a high ultimate stress to yield stress ratio of the steel. These material properties such as yield stress and ultimate to yield stress ratio may or may not have much effect on the strength at 1/4 in. hole elongation. Little attempt to understand the influence of the steel material properties on the strength at 1/4 in. displacement has been made.

There is the other type of bolted shear connections where the force is transferred from one member to the other member via not only the bolt shear force but also by the frictional force on the contact surface. This frictional force is proportional to the normal force which comes from the tension in the bolt. At the initial stages of loading, the load is transferred by the friction between surface of the members. When the shear force is larger than the resisting force which can be developed by the friction, then slip occurs and the bolts bear on the edge of hole. Therefore, the force is mainly transmitted through bearing and through the shear force in the bolt after the slip occurs since there is little frictional force. Usually, this frictional force is not reliable after slip occurs. As a result, the strength after slip is estimated only by the shear strength of the bolt and the

bearing strength. This provides a lower bound limit of the strength of the bolted shear connections at failure. Most of the test data available is based on experiments with friction. Even for tests where the bolt is just snug-tightened, there is a frictional force between the members at the failure of the connection. The yielded material piles up around the bolt hole as the hole elongates. When the pile-up is confined between bolt heads and nuts, a frictional force develops due to the contact pressure in the area where the pile-up of material increases the thickness. Since the strength without any frictional force is a good measure of the lower limit of the strength of bolted shear connections, the lower limit of the strength can be obtained by providing a gap so that the material can pile up without inducing any frictional force.

1.2 Previous Research

Many tests on bearing strength have been done with light gage steel because the bolts tend to shear off before the bearing strength is reached for bolted shear connections with thick connected members. An experimental study on single bolted connections in light gage steel was undertaken by Winter[11]. The program included a wide range of material properties with the ultimate stress to yield stress ratio from 1.2 to 1.6 approximately. Bolts were torqued. Based on the test results, an end distance of 3.5d was adopted as a dividing line between end tearout failure and bearing failure. It was determined that the strength of the connection was $1.4L_etF_y$ for the end tearout failure and was $4.9dtF_y$ for the bearing failure with a considerable pile-up of the material in front of the bolt. Yield stress of the material rather than the ultimate stress was used since it was considered through the preliminary investigation before the test that better predictions could be achieved with the yield stress of the material rather than with the ultimate stress. Most of the test results were in the range of 80% to 120% of these strength prediction. It was mentioned in the report that the failure load was only slightly affected by curling of the free end of the connection and that the strength at 1/16 in. displacement did not show any consistency. For the tests using the strength at 1/16 in. displacement, bolts were initially in bearing with the holes before the torque was applied

in the bolts.

The strength of bolted connections in light gage steel was also investigated by Chong and Matlock[3]. Compared with the tests by Winter, the test specimens did not have any washers under the heads of the bolts and the nuts. But, the bolts were also torqued to the standard torque as done by Winter. The ultimate stress to yield stress ratio of material ranged from 1.1 to 1.5. The results showed that the strength without washers was about 45% less than the strength with washers. The strength was $1.08L_etF_y$ for end tearout failure and $2.7dtF_y$ for bearing failure depending on the end distance. An end distance of 2.5d was used as the dividing line between the end tearout failure and the bearing failure. The curling and bending of the free end of the plate was again reported to have negligible effect on the strength.

Discussion on the tests by Chong and Matlock was made by Haussler and Pabers[6]. In this discussion, the test results for 0.0236 in. thick material with various bolt torques were also presented. It was shown that the use of a washer and torque significantly increase the strength.

Tests on thin light gage bolted connections without washers were conducted by Gilchrist and Chong[5]. Bolts were torqued to a standard torque and washers were not used. The failure load was reported to be $0.96L_etF_y$ for L_e less than or equal to 2.5d and to be 2.4 dtF_y for L_e more than 2.5d. The test results fell mostly in the range of the 80% to 120% of the proposed strength predictions. It should be noted that similar scatter was observed when ultimate stress instead of yield stress was used for the strength prediction. The strength predictions based on the ultimate stress F_u were $0.84L_etF_u$ and $2.1dtF_u$ respectively. Material in the tests had ultimate to yield stress ratio of around 1.15. The equations above were for steels with 22 , 24, and 26 gage thickness. The strength of connections with light gage steels with 12, 14, 16, 17, and 20 gage thickness were reported by Chong and Matlock as mentioned above. Very thin light gage steel bolted connections showed a lower strength than light gage steel bolted connections with thicker material.

Tests on the strength of single angle, single bolted connections were done by

Kennedy and Sinclair[7]. The primary objective was to determine the capacity of 5/8 in. thick single angle, single bolted connections which were commonly used for tower structures. So as to give the clamping force as the force in the connections in tower structures, bolts were torqued. By applying a load of 200 to 400 lb before torquing the bolts, slip in the connection was eliminated. Therefore, the test specimens were different from slip critical connections since bolts could not slip. The mean ultimate stress to yield stress ratio of the material was 1.393. But, the material properties of individual specimens varied. Because the angle could fail in either end tearout or in edge fracture, different equations were given for these two types of failure. The strength of the connections was reported as a function of thickness, end distance, edge distance and yield stress. The failure bearing stress was reported to be about 4.5 times the yield stress of the material. This is about 3.23 times ultimate stress of the material considering ultimate stress to yield stress ratio of 1.393. It was shown that the ratio of the normalized strength with ultimate stress to the normalized strength with yield stress is same as the ratio of ultimate stress to yield stress of material. That is, either ultimate stress or yield stress could be used in the strength predictions. The strength was about $(1.257L_e+.174)\ tF_y$ for end tearout failure.

Frank and Yura reported the effect of bearing ratio and lateral confinement on the bearing strength of bolted shear connections[4]. The bearing ratio was defined as the ratio of bearing stress to the net section stress. Since the force term in the bearing stress and the net section stress cancel each other, the bearing ratio becomes a geometric factor. Symmetric lap splices made of 1/4 in. A36 steel plate with round or slotted holes were tested and the A36 steel had an ultimate to yield stress ratio around 1.45 to 1.5. It is reported that the presence of the net section stress decreased the bearing strength at failure and that the laterally confined members such as the inside splices of the connections reach higher bearing strength at failure than those with less or no confinement. This was a different result from the results of early research by Winter and by Chong and Matlock, where it was reported that the curling of free end had negligible effect on the strength. Strength at 1/4 in. hole elongation was also examined as a failure criteria. It

was shown that fully torqued bolts had 10% more strength compared with the sung tight connections when the 1/4 in. hole elongation criteria was employed. The results are detailed in the thesis written by Perry[10].

Lewis reported the results of forty eight single bolted connection tests and fifty three double bolted connection tests[9]. Tested material was A36 steel with ultimate stress to yield stress ratio around 1.4 to 1.5 and the tests were conducted with various clear distance, spacing, plate thickness, and bolt diameter. The frictional force was eliminated by providing a gap between the specimen and the test fixture. Various design equations were checked with these test results. Lewis reported that current AISC-LRFD design equations give accurate strength predictions for single bolted connection while they are inadequate for multi-fastener connections. When spacings are not less than 3.0d, the bearing strength at the hole closest to the end is predicted to be $L_e tF_u$ for the end distance less than 1.5d, and to be 2.4dtFu for the other end distance in the current AISC-LRFD design equations. There is a discontinuity in the strength predictions at an end distance of 1.5d since the replacement of L_e with 1.5d results in the strength prediction of $1.5dtF_u$ which is less than $2.4dtF_u$. This discontinuity in the equations was reported by Lewis to be unnecessary. Lewis also said that the proposed clear distance approach[12] was considered to be conservative based on the test results.

1.3 Objectives and Scope

The test program used one-bolt and two-bolt lap splices. Nuts were removed so as to avoid the development of any frictional force between the splices. For one-bolt lap splices, bolt holes were made with the clear end distance of 0.5d, 1.0d 1.5d and 2.0d, where d is the diameter of the bolt. The two-bolt lap splices had clear end distances of 0.5d and 1.5d with the combinations of the clear spacings between the bolts of 1.0d, 2.0d, and 3.0d. Short clear distances such as 0.5d and 1.0d were chosen to induce the end tearout failure mode. And, moderate clear distances such as 1.5d end distance with 3.0d spacing was selected to provide bearing type failures.

Main objective of the test program is to study the influence of the material

properties on the strength of bolted shear connections. Two heats of steel were selected to see the difference in behavior. One had high ultimate stress to yield stress ratio and the other had low ultimate stress to yield stress ratio. One-bolt connections were tested with each heat of steel through AO and BO test series, and tests on two-bolt connections were conducted through AT and BT test series. The strength with regard to end distance and spacing was compared with the current design equations and the proposed clear distance design equations.

In Chapter one, general background knowledge has been introduced and the previous research work discussed. In Chapter two, the experimental setup and the instrumentation used in the test program are described in detail. In Chapter three, test results are presented with discussion, followed by the observations made during the test. In Chapter four, comparison of the test results with the existing design equations and with the previous research is made. Conclusions are presented in Chapter five.

CHAPTER 2

Test Program

This chapter describes the experimental program to study the effect of the yield and the ultimate stress of the steel on the strength associated with the end tearout failure mode and the bearing failure mode of the bolted lap splices. A test fixture and a displacement measuring device are explained and test procedures are described in detail. In the test program, eight preliminary tests with one-bolt lap splices were conducted through the AW test series to study the effect of the width of the splice. Then, eighteen tests were conducted with steel plates of a high ultimate to yield stress ratio through the AO and AT test series. Six of these had one bolt hole and the others had two bolt holes. Nineteen tests were done with steel plates of a low ultimate to yield stress ratio through the BO and BT test series. Eight of these had one bolt hole and the others had two bolt holes. Three quarter inch bolts were used to connect the splices with standard 13/16 in. holes in the plates. Nuts were not used on the bolts to eliminate the friction between the splices.

2.1 Test Variables

In AW test series, widths of the specimen was varied while maintaining the end distance of the bolt hole and the material property of the steel plates.

In AO, BO, AT, and BT test series, ultimate to yield stress ratio was the main variable. Two heats of steel were used in the test series. The one had a high ultimate to yield stress ratio and the other had a low ultimate to yield stress ratio. End distances and spacings were varied with each heat of steel to see the difference in behavior due to the material property at various end distance and spacing.

2.2 Specimen

Preparation of the Specimen

Test plates were originally sheared to be 3 to 6 in. wide and 3 to 6 feet long at

the beginning. A bolt hole was punched for each specimen at one end of the plate and the other end was to be gripped by the test machine. After each test, tested portion of the plate was cut off and another hole was punched for the next test as shown in Figure 2-1. It was assumed that the tested portion of the plate would not affect the strength of the specimen at the next test which is conducted with the remaining portion. This assumption would be valid as long as the stress in the gross section of the specimen is in elastic range and the yielded portion around the hole of the tested specimen was cut and cleared from the portion to be tested in the next test. It was possible to have the localized yielding around hole propagate up to more than 2 or 3 inches toward the remaining portion. So as to clear this yielded area for the next test, the surface of the specimen was carefully studied after each test and the cut was made about 3 to 6 inches above the hole of the tested specimen.

Since the test plates were originally sheared, the first specimen of the plate had the sheared end. The cut in the plate was made by a band saw for the next specimen. Therefore, the other specimen of the plate had the sawed end.

Geometric Configuration

Plates used in the test program were nominally 3/16 in. thick. Specimens in AW test series had nominal widths of 3, 3.5, 4.5, and 6 inches as shown in Figure 2-3. The hole was made with a clear end distance of 1.2 in. from the end of the specimen to the edge of the hole.

Specimens in the AO, and BO test series were nominally 3.5 in. wide and had one hole. Nominal clear end distance of the hole was varied from 0.5d to 2d in 0.5d increments, where d was the diameter of the bolt. This is shown in Figure 2-4.

Each specimen in the AT and BT test series had a nominal width of 6 in. and had two holes. The hole close to the end of the specimen had a nominal clear end distance of either 0.5d or 1.5d. The nominal clear spacing between the holes was varied from 1.0d to 3.0d in 1.0d increments with each clear end distance as shown in Figure 2-5.

For all the specimens, 3/4 in. diameter A490 bolts were used to resist the single

shear stress. Accordingly, 13/16 diameter standard holes were made in the specimen. A few of the holes were drilled and the others were punched. Since only three specimens had drilled holes, distinction between the punched and the drilled hole was not made. For the specimen where the hole was drilled, there was no difference between the diameter of the hole on one side and on the other side. But, for those where the hole was punched, there was slight difference in the hole diameter as shown in Figure 2-2. The diameter of the hole on the front side where the punch was applied was accurate but the diameter of the hole on the back side was slightly larger. Therefore, the clear distance measured on the front side was also slightly larger than the distance on the back side.

Material Properties

Two heats of steel were used in the test program. So as to obtain the yield stress and ultimate stress of each heat of steel, three tension coupons conforming to the ASTM A370 standard were made from each heat of steel and the actual width and thickness were measured. Coupon tests were conducted on a calibrated universal test machine. Static values of the strength were obtained by recording the load after stopping the straining for four minutes. The static values of load were measured three times on yielding plateau and once at ultimate. Static stresses and dynamic stresses were calculated by dividing the strength by the cross sectional area and are listed in the Table 2-1. One heat of steel was named material A, and the other was named material B.

Material A had a static yield stress of 38.7 ksi, a static ultimate stress of 62.3 ksi and a percent elongation of around 30%. Material B had a static yield stress of 70.1 ksi, a static ultimate stress of 79.1 ksi and a percent elongation of 18%. Dynamic stresses were about 4% to 7% higher than static stresses. Two of coupon test results are plotted in Figure 2-6. Main difference of these two material considered in the test program was the ultimate to yield ratio. The material A is considered to have ductile behavior while material B is considered to be brittle, as is also shown by the comparison of percent elongation of each material.

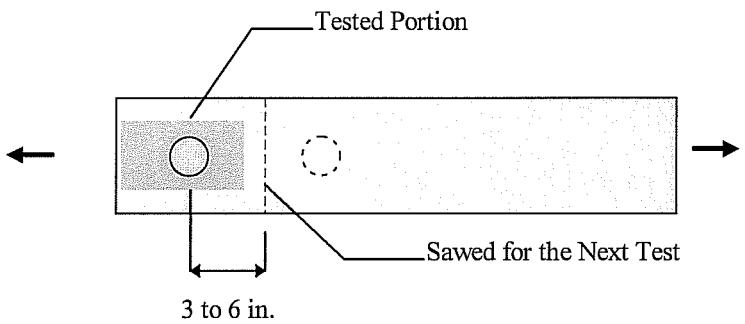

Figure 2-1 Preparation of the Test Specimen

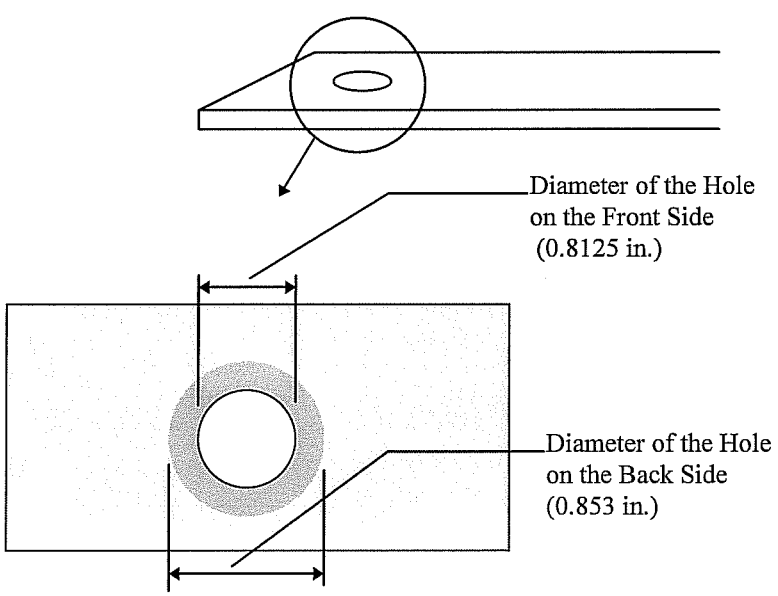

Figure 2-2 Diameter of the Punched Hole

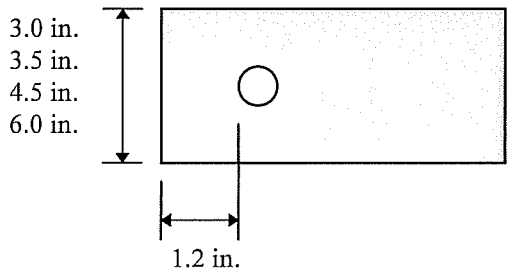

Figure 2-3 Specimen for AW Test Series

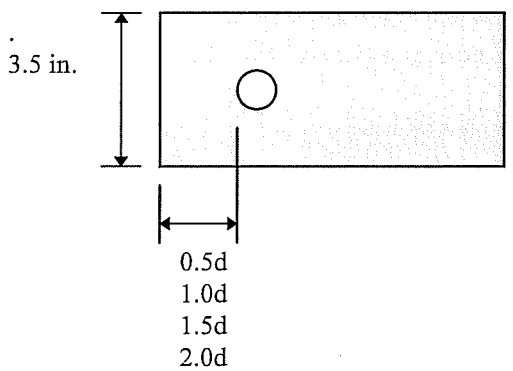

Figure 2-4 Specimen for AO and BO Test Series

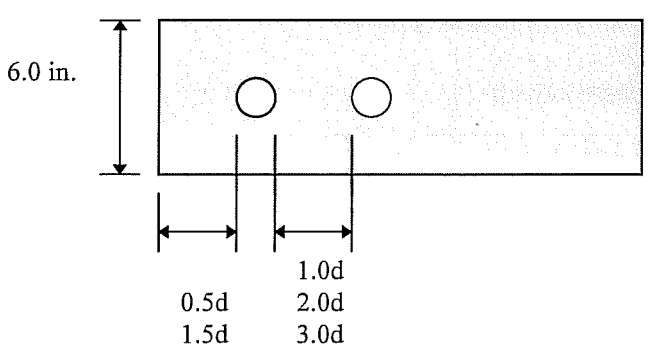

Figure 2-5 Specimen for AT and BT Test Series

Table 2-1 Material Properties

Material A

Unit: ksi

	Static Yield	Static Ultimate	Dynamic Yield	Dynamic Ultimate	Percent Elongation
Coupon 1	38.47	62.27	41.26	65.21	28.9%
Coupon 2	38.98	62.41	41.49	65.56	29.4%
Coupon 3	38.69	62.34	41.44	65.44	30.1%
Average	38.71	62.34	41.40	65.40	
Standard Deviation	0.26	0.07	0.12	0.18	

Material B

Unit: ksi

	Static Yield	Static Ultimate	Dynamic Yield	Dynamic Ultimate	Percent Elongation
Coupon 1	69.54	77.66	71.94	81.72	NA
Coupon 2	70.96	79.82	73.86	83.68	18.8%
Coupon 3	69.76	79.94	72.85	81.86	17.5%
Average	70.09	79.14	72.88	82.42	
Standard Deviation	0.76	1.28	0.96	1.09	

Summary

Unit: ksi

	Material A	Material B
Static Yield	38.71	70.09
Static Ultimate	62.34	79.14
Static Ultimate / Static Yield	1.61	1.13

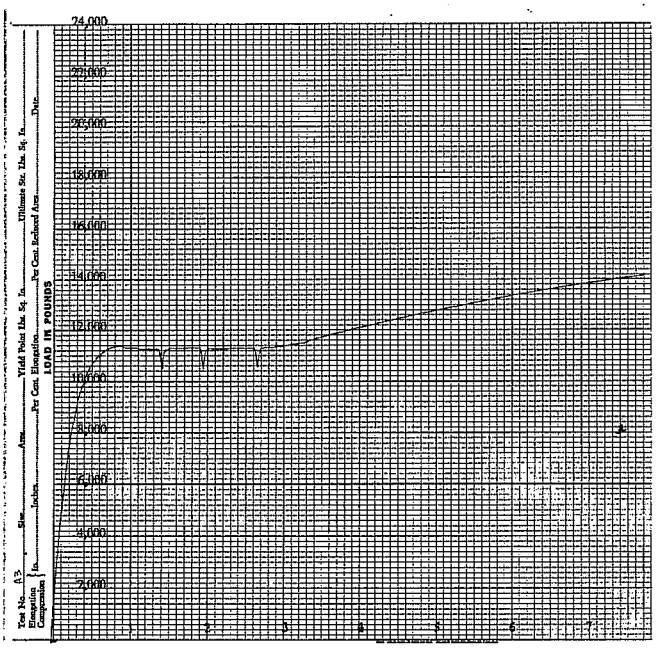

(a) Load-Displacement Curve of Material A

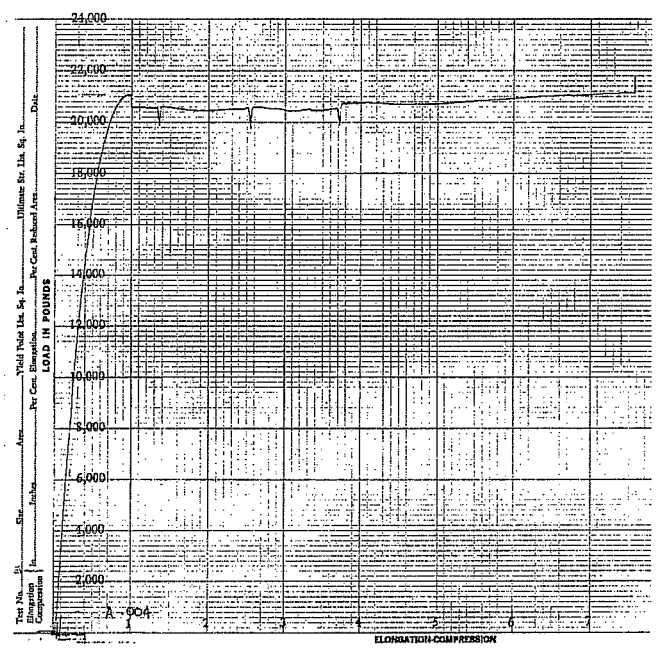

(b) Load-Displacement Curve of Material B

Figure 2-6 Coupon Test Results

2.3 Test Setup

The loading fixture was made of two plates as shown in Figure 2-7 and Photo 1. One had 2 in. thickness and the other one had 5/8 in. thickness. A 3/4 in. diameter hole was drilled in the 2 in. thick plate and a 3/4 in. diameter A490 bolt with which the test specimen would be connected was inserted. The 3/4 in. diameter hole was considered to be snug enough to restrain any tilting of the bolt as shear was applied. A 5/8 in. thick plate was selected to keep the loading applied by the test machine acting through the centerline of the specimen. Two A490 bolts and two A325 bolts which had 7/8 in. diameter were used to fasten these two plates together. These bolts were tightened using the turn of the nut method. A 3/16 in. gap between the fixture and the specimen was originally intended to provide free space which would eliminate any friction on the surface.

This original configuration had minor modification through the test program when unexpected behavior of the test specimen occurred. These modifications and the characteristics of the behavior are discussed later.

2.4 Measurements

Geometric configurations of each specimen were measured with a caliper. For a few specimens, the diameter of hole was also measured. For specimens with punched holes, the clear distances on the front side where the punch was applied was measured and used throughout the test program. Even though the diameter of hole on the front side was different from that on the back side, no attempt to average these distances was made. The difference is small and the usual measurement of the end distance and spacing would be close to the distance on the front side.

A small device with a linear potentiometer was used to measure the deformation. As shown in Figure 2-8, four small bolts gripped the potentiometer mount to the specimen at two points on each side along a transverse line perpendicular to the line of applied loading. The gripping area was small enough not to interfere with the deformation of the specimen. The deformation measured by the linear potentiometer

consists of a) Elastic and plastic deformation due to bearing around the bolt hole.

b) Elastic and plastic deformation of the net section.

c) Elastic deformation of the gross section from the top edge of the hole to the line where the device is attached.

2.5 Test Setup Modifications

Modification 1

For specimen AW45R, the following modifications were made in the test setup. A small clamping device was fabricated, and installed on the 3/4 in. diameter bolt as shown in Figure 2-9. The role of clamping device was to restrain a small area around the hole in the specimen from moving out of plane. The small bolt used in this clamping device held the position of the clamping device until the build up of material around hole pushed the clamping device outward. The clamping device provided some lateral restraint to the specimen. A plastic shim was inserted between the specimen and the clamping device so that only a small area of the specimen was in contact with the clamping device. The 3/16 in. wide gap between the specimen and the test fixture was eliminated.

Modification 2

For specimen AW45S, another modification was made as shown in Figure 2-10. The plastic shim was removed to increase the contact area and provide more lateral restraint to the specimen. The restraint was required because the initial crookedness of the specimen plate made a gap between the specimen and the test fixture. This gap was removed by applying a lateral force as shown in Figure 2-11 until the specimen was in tension from the applied loading of the test machine.

For most of the specimens tested, this clamping device was used to restrain lateral movement of the specimen. For a few specimens with a short end distance, where the clamping force was not necessary, the clamping device was not used and the potentiometer was placed back on the 2 in. fixture plates shown in Figure 2-12.

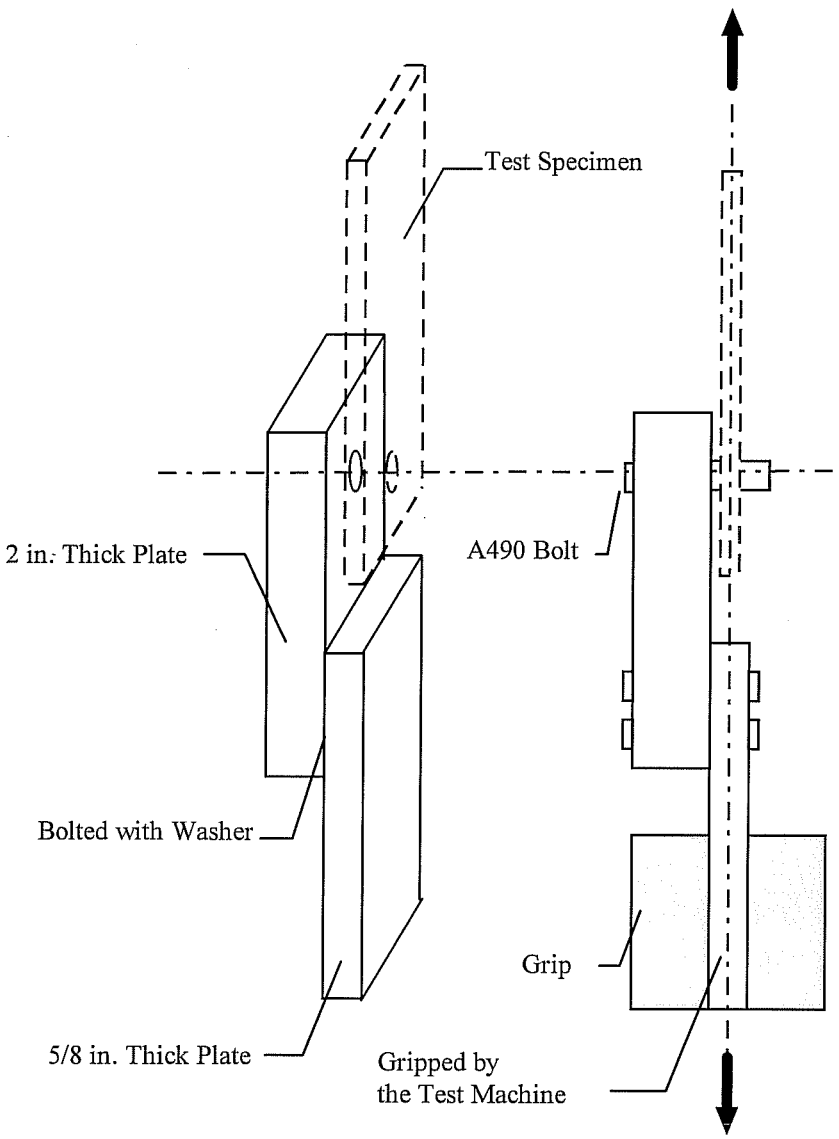

Figure 2-7 Test Setup

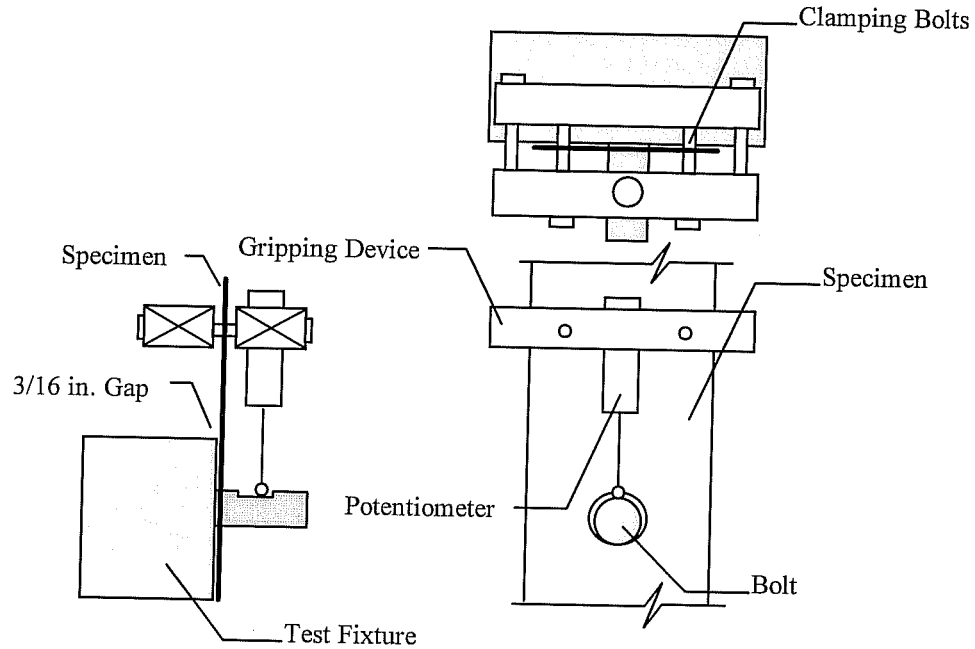

Figure 2-8 Displacement Measurement

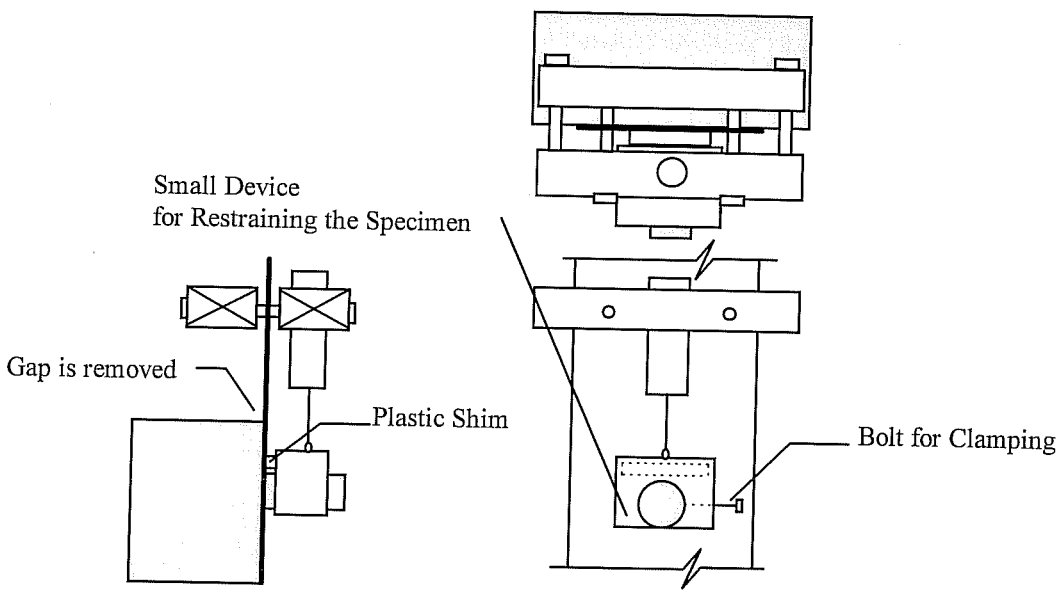

Figure 2-9 The Clamping Device : Modification 1

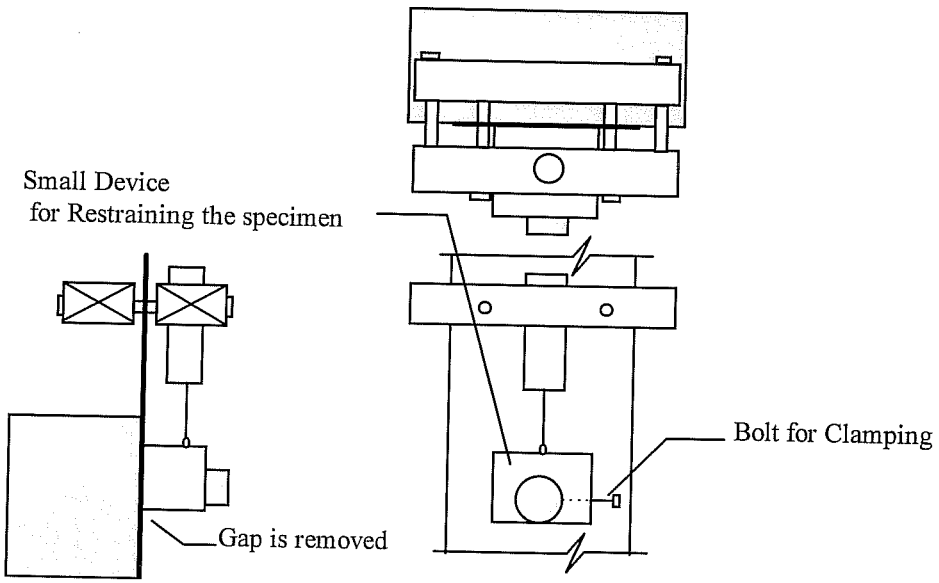

Figure 2-10 The Clamping Device : Modification 2

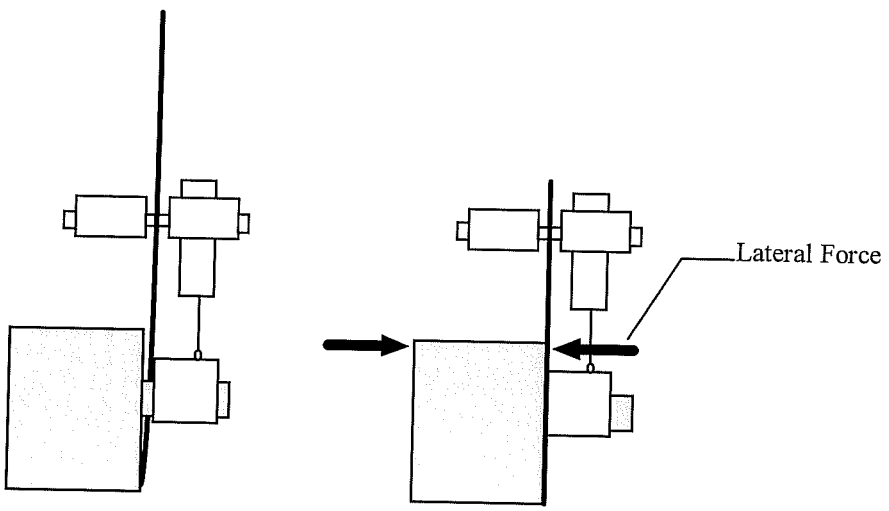

Figure 2-11 Initial Crookedness and the Lateral Force

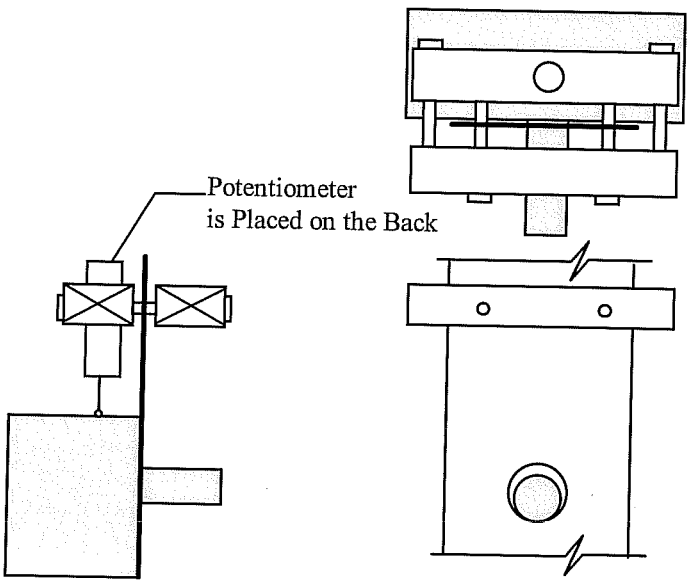

Figure 2-12 Displacement Measurement 2

2.6 Test Procedure

Before the test, all specimen dimensions were measured with a caliper. Then, the surface of the specimen was whitewashed so that yield lines could be seen clearly during the test. The specimen was put in the testing machine, and was bolted with the test fixture. No nuts were used on the test bolts. The displacement measuring device was mounted on the specimen. The load was applied by test machine up to approximately 5% of the elastic range and the load was slowly removed until the load reading became zero. The intention was to make the bolt bear on the edge of the hole for the initial readings. Load was then applied and the static values of the load were obtained by stopping the straining for four minutes at several points on the load-deformation curve. Photos were taken at various stages of loading. The load-displacement curve was automatically recorded by the data acquisition system. When the load dropped significantly due to the failure of the specimen, the test was stopped, and the specimen was dismantled from the fixture. The test portion of the plate was cut off using a band saw. A hole was then punched for the next test.

2.7 Calculations

The linear potentiometers were calibrated before the tests. Calibration factors were obtained for every potentiometer used in the tests and they were used to correct the recorded displacement into the actual displacement.

Elastic deformation of the net section and the gross section shown in Figure 2-13 was calculated based on the thickness and width of the specimen and the elastic modulus. For simplicity, a uniform stress distribution was assumed for the calculation, and the width of the net section was assumed to be the width of the specimen minus the diameter of the bolt hole. These calculated elastic deformations were subtracted from the total deformation measured by the potentiometer. Compared with the plastic deformation due to the bearing and the net section stress, the elastic deformation was only a few percent of the total deformation.

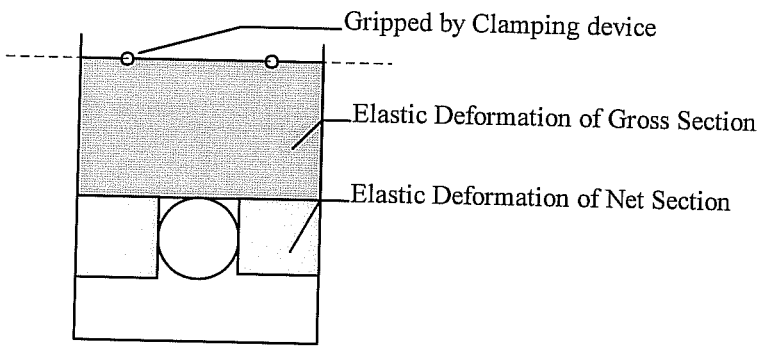

Figure 2-13 Elastic Deformation

Due to the stress concentration, yielding of the net section starts close to the bolt hole. For specimens with a small width, yielding around the hole can propagate to the edge and the whole net section can have a large plastic deformation. If the plate is wide enough, yielding of the net section is restricted to the small area around the hole. Therefore, yielding of the whole net section can be avoided if enough width is used. But, the localized yielding around the bolt hole in the net section can not be avoided even though the specimen is wide. The yielding would occur for any net section with any width. Therefore, the plastic deformation due to the yielding around the hole in the net

section was considered to be a part of the bearing deformation and was not subtracted from the total displacement. If the whole net section deforms, the plastic deformation should be calculated and subtracted from the total deformation.

Detailed descriptions on the calculations are given in Appendix.

2.8 Problems Associated with the Measurement

The initial crookedness of the plate could cause out-of-plane rotation of the deformation device and the potentiometer when the specimen straightened under tensile loading. These rotations could increase or decrease the measured displacement. For most of the specimens, the crookedness was not so severe and the crookedness in the tested portion was minimized by applying lateral force. Therefore, displacement due to out-of-plane rotation was considered to be small and was disregarded.

A small clamping device was used for many specimens as mentioned before. When the load increased the device could rotate in plane as shown in Figure 2-14. But, the rotation was small and the error induced by the rotation was considered to be around 2 or 3% of total displacement. For most specimens, the rotation did not occur. When the potentiometer was installed on the back side of the specimen, the rotation did not affect the displacement measurement. Therefore, the error due to the rotation of the clamping device was disregarded.

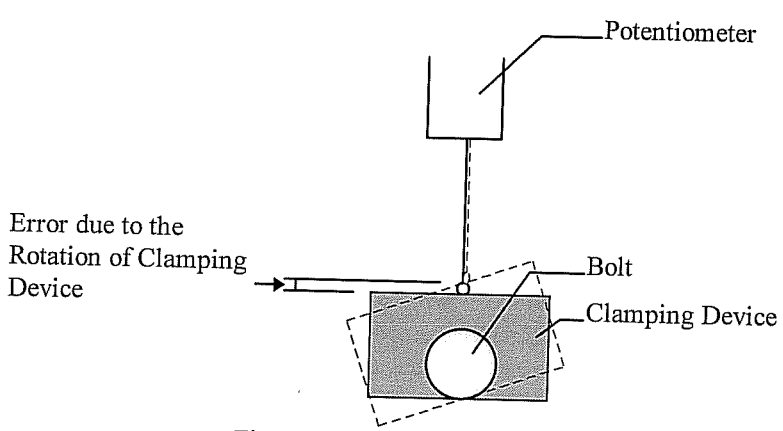

Figure 2-14 Rotation of the Clamping Device

2.9 Notation

The first character in the specimen designation represents the material property of the connected members. Two materials were used in the tests. One had high ultimate to yield ratio and the other had low ratio. The one with a low ultimate to yield ratio was designated material A and the other was designated material B.

The second character represents whether the specimen had one bolt or two bolts. O represents one-bolt connections and T represents two-bolt connections. For the specimens which were tested with various widths, W was used instead of O even though they had one bolt. For example, the AW test series means that the test specimens from material A have various widths. The BT test series means that the test specimens from material B have two bolts. There are only five test series; AW, AO, BO, AT, and BT.

Numbers in AW test series designation represent the width of the specimen. Numbers in other test series represent nominal clear end distances or/and nominal clear spacing normalized with the factor of d, where d is the diameter of bolt. For one-bolt connections, the first two digit number represents nominal clear end distance. For two-bolt specimens, the first two digit number represents nominal clear end distance and the next two digit number represents clear spacing.

For the replicates, character R was attached at each end of the designation. For additional tests beyond the replicate, other character such S or U was attached instead of R. For example, AW450 had a nominal width of 4.5 inches. AT0520R was the replicate of AT0520 which had a nominal clear end distance of 0.5d and a nominal clear spacing of 2.0d.

CHAPTER 3

Test Results

Load-displacement data were recorded by the data acquisition system. The measured displacements from the potentiometer were corrected by multiplying by calibration factors. Then, the elastic deformations of the net section and gross section based on the assumed dimension were calculated and were subtracted from the total displacement. Using this modified displacement data, a load-displacement curve was generated and the load at 1/4 in. displacement and the load at ultimate were obtained as shown in Figure 3-1. Dynamic values of the strengths were used since the differences between the dynamic and the stactic values were small. When the maximum strength was reached before the hole elongated 1/4 in., the maximum strength was used for the strength at 1/4 in. displacement instead of actual strength at 1/4 in. displacement.

The results from the AW test series where width was varied are presented first, followed by the results of the tests on the one-bolt and the two-bolt connections. The failure modes of the specimens in each test series are described. The effect of using F_y or F_u to characterize the behavior is discussed.

3.1 Results

The actual dimensions of the specimens and the test results are listed in Table3-1. Specimens that buckled during the test are not listed. In the table, C1 is the clear distance measured along the line of force from the edge of the hole to the end of the connected member and C2 is the clear spacing measured from the edge of the hole to the edge of the adjacent hole. The strength at 1/4 in. displacement and the strength and displacement at ultimate are listed. Strength predictions by AISC-LRFD[1] and by a clear distance approach[12] are also listed. In the table, $P_{1/4,\ LRFD}$ and $P_{1/4,\ Clear}$ are based on the equations for the case where deformation around the bolt holes is a design consideration, and $P_{u,\ LRFD}$ and $P_{u,Clear}$ are the strength predictions which can be used when deformation around the bolt holes is not a design consideration.

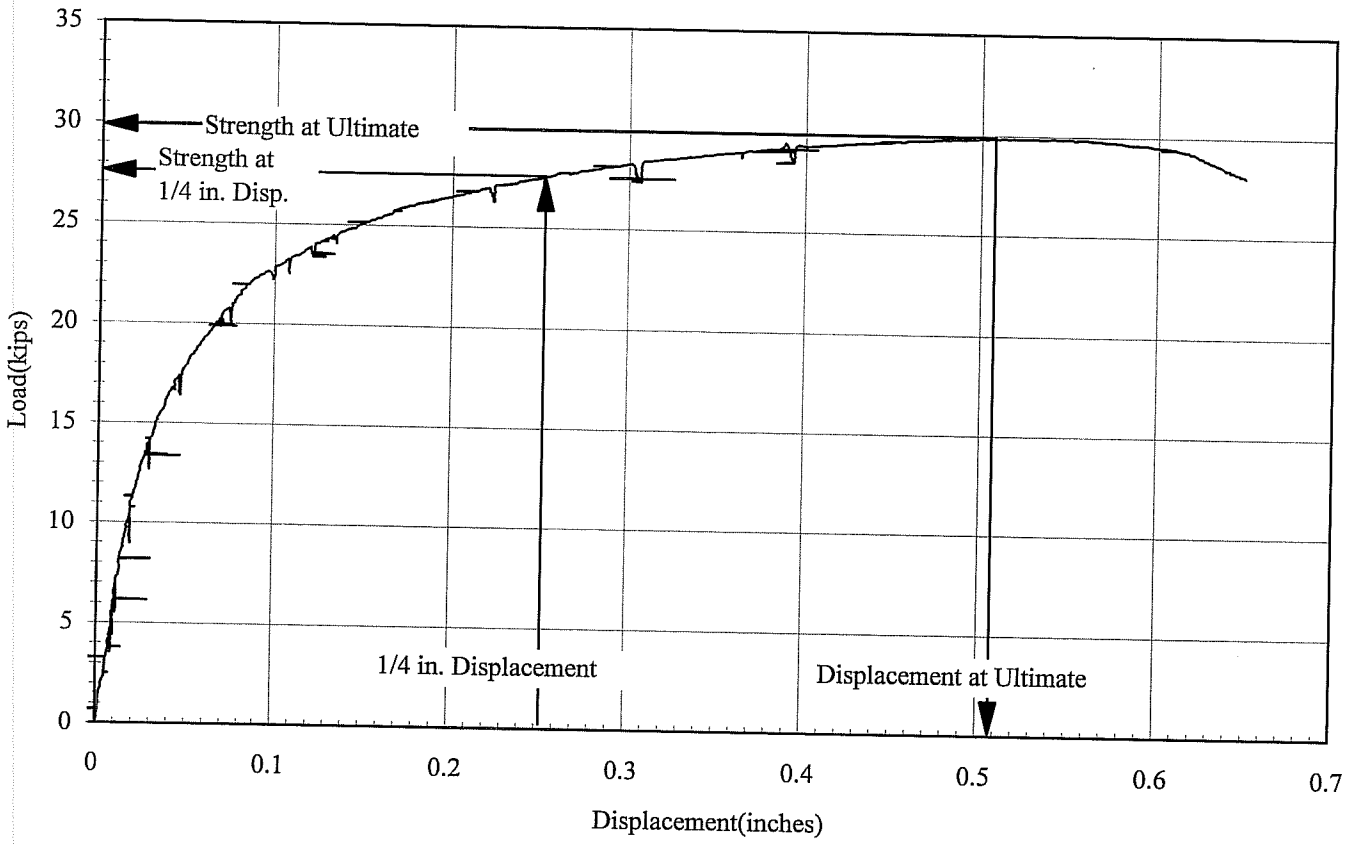

Figure 3-1 Plot of Modified Displacement and Load Data(BO200)

Table 3-1 Test Results

Specimen	C1	C2	w	t	F_y	F_u	$P_{1/4}$	P_u	$Delta_u$	$P_{1/4, LRFD}$	$P_{u, LRFD}$	$P_{1/4, Clear}$	$P_{u, Clear}$
AW300	1.20	-	3.00	0.182	38.7	62.3	18.2	20.0	0.42	18.2	-	16.3	-
AW350	1.23	-	3.53	0.183	38.7	62.3	18.5	19.5	0.37	18.6	-	16.8	-
AW35R	1.23	-	3.53	0.182	38.7	62.3	18.6	19.9	0.40	18.6	-	16.7	-
AW45S	1.24	-	4.54	0.183	38.7	62.3	19.5	20.3	0.42	18.7	-	16.9	-
AW45U	1.18	-	4.54	0.183	38.7	62.3	18.2	20.0	0.47	18.1	-	16.2	-
AW600	1.22	-	5.95	0.182	38.7	62.3	19.1	20.2	0.34	18.4	-	16.6	-
AO050	0.36	-	3.54	0.183	38.7	62.3	8.5	8.5	0.19	8.7	-	4.9	-
AO050R	0.36	-	3.53	0.183	38.7	62.3	8.6	8.6	0.21	8.8	-	4.9	-
AO100	0.74	-	3.54	0.184	38.7	62.3	13.7	13.8	0.27	13.1	-	10.2	-
AO150	1.12	-	3.53	0.183	38.7	62.3	16.7	18.2	0.52	17.4	-	15.4	-
AT0510	0.37	0.76	5.99	0.183	38.7	62.3	22.8	22.8	0.23	22.5	-	15.4	19.3
AT0510R	0.37	0.76	5.96	0.182	38.7	62.3	23.6	23.9	0.30	22.3	-	15.3	19.1
AT0520	0.36	1.32	5.96	0.182	38.7	62.3	26.0	27.1	0.33	28.6	-	22.8	28.5
AT0520R	0.38	1.31	5.99	0.183	38.7	62.3	26.5	27.9	0.34	28.9	-	23.1	28.9
AT0530	0.36	2.20	5.97	0.182	38.7	62.3	27.5	27.5	0.21	29.1	-	25.3	31.6
AT0530R	0.38	2.18	5.96	0.183	38.7	62.3	28.3	28.6	0.27	29.5	-	25.7	32.1
AT1510	1.09	0.74	5.96	0.183	38.7	62.3	31.0	32.8	0.40	30.5	-	25.1	31.4
AT1510R	1.11	0.76	5.98	0.183	38.7	62.3	31.6	34.3	0.47	31.0	-	25.7	32.1
AT1520	1.09	1.33	5.99	0.182	38.7	62.3	33.9	38.6	0.57	37.1	-	33.0	41.2
AT1520R	1.13	1.30	5.96	0.181	38.7	62.3	34.5	39.4	0.58	37.0	-	32.9	41.2
AT1530	1.17	2.20	5.98	0.183	38.7	62.3	37.0	39.9	0.37	41.1	43.6	36.5	45.7
AT1530R	1.13	2.20	5.98	0.183	38.7	62.3	36.9	45.1	0.69	41.1	43.1	35.9	44.9
BO050	0.36	-	3.55	0.187	70.1	79.1	11.1	11.1	0.25	11.3	-	6.4	-
BO050R	0.39	-	3.55	0.187	70.1	79.1	11.9	11.9	0.23	11.7	-	6.9	-
BO100	0.74	-	3.61	0.189	70.1	79.1	17.9	18.1	0.33	17.2	-	13.3	-
BO100R	0.73	-	3.61	0.188	70.1	79.1	18.1	18.4	0.30	16.9	-	13.1	-
BO150	1.13	-	3.61	0.188	70.1	79.1	23.1	24.3	0.48	22.8	-	20.1	-
BO150R	1.13	-	3.56	0.187	70.1	79.1	24.5	25.2	0.37	22.7	-	20.1	-
BO200	1.51	-	3.61	0.187	70.1	79.1	27.5	29.9	0.51	26.6	-	26.6	-
BO200R	1.47	-	3.54	0.187	70.1	79.1	27.4	29.9	0.62	26.6	-	26.1	-
BT0510	0.35	0.75	6.04	0.187	70.1	79.1	32.1	32.8	0.35	28.7	-	19.5	24.4
BT0510R	0.36	0.74	6.09	0.188	70.1	79.1	32.1	32.9	0.37	28.9	-	19.7	24.6
BT0520	0.36	1.31	6.09	0.188	70.1	79.1	35.8	38.4	0.48	37.4	-	29.8	37.2
BT0520R	0.35	1.31	6.03	0.187	70.1	79.1	36.9	39.0	0.41	37.0	-	29.4	36.8
BT0530	0.31	2.19	6.05	0.187	70.1	79.1	39.5	43.0	0.43	37.2	-	32.1	40.2
BT0530R	0.36	2.18	6.10	0.187	70.1	79.1	40.0	44.6	0.45	37.9	-	33.0	41.2
BT1510	1.10	0.75	6.10	0.188	70.1	79.1	43.1	44.6	0.38	40.0	-	32.9	41.2
BT1510R	1.11	0.75	6.03	0.187	70.1	79.1	43.5	45.4	0.43	40.0	-	33.0	41.3
BT1520	1.09	1.31	6.03	0.188	70.1	79.1	46.8	50.7	0.52	48.2	-	42.8	53.5
BT1530	1.17	2.20	6.10	0.187	70.1	79.1	50.2	57.1	0.53	53.3	56.6	47.4	59.2
BT1530R	1.10	2.18	6.05	0.187	70.1	79.1	51.4	60.2	0.77	53.3	55.6	46.2	57.7

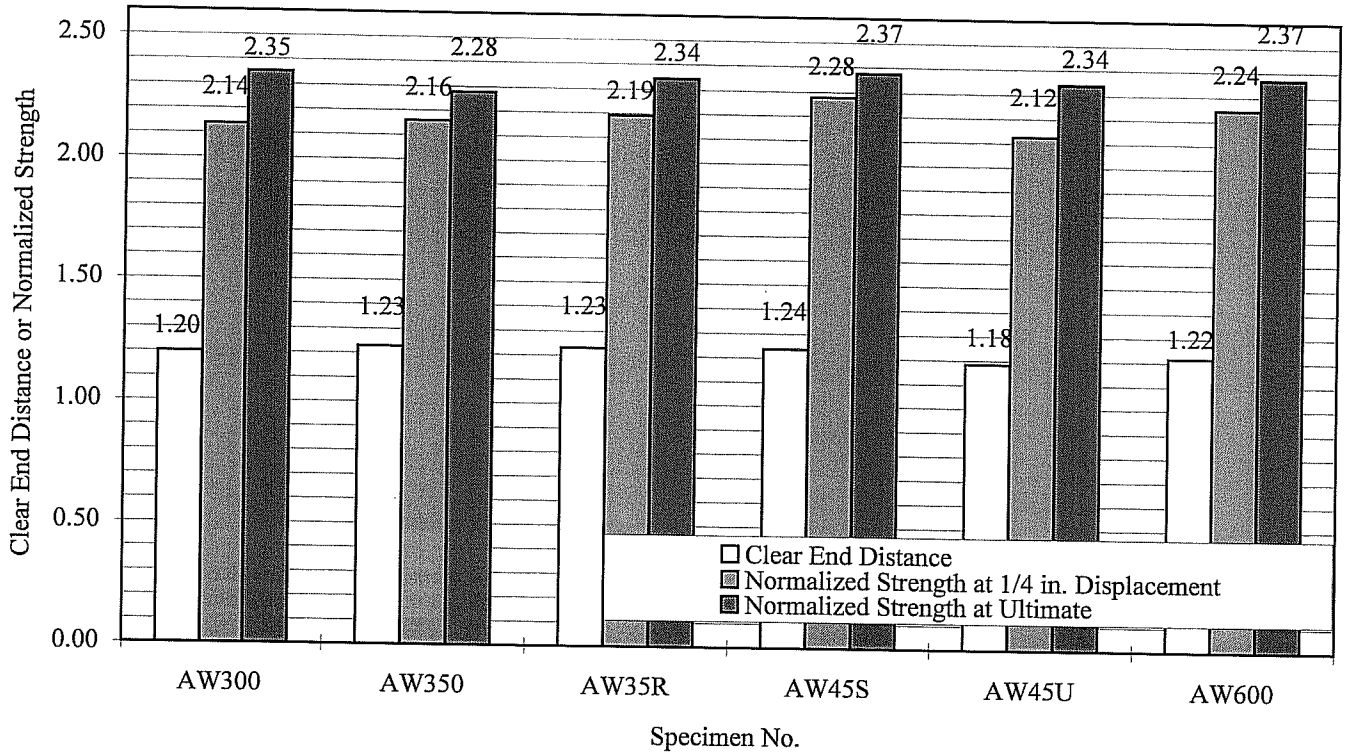

Figure 3-2 Effect of Width on One Bolt Specimen

3.1.1 AW Test Series

Effect of Width

The results of AW test series are summarized in Figure 3-2. The clear end distances differ slightly from specimen to specimen, but they are within a 5% range. The strength at 1/4 in. displacement and the strength at ultimate are shown in the figure. These strengths are normalized with dtF_u. The clear end distance of the 3 in. wide specimen differs from the clear end distance of 6 in. wide specimen by only 2%. Both the strengths of 3 in. wide specimen at 1/4 in displacement and at ultimate differ by less than 5% from those of 6 in. wide specimen. Even though the bearing ratio of the 3 in. wide specimen is much lower than that of the 6 in. wide specimen, the net section stress did not affect the bearing strength of the specimen with the selected clear end distance of 1.2 inches.

Since the 3.5 in. wide specimens in AW test series do not show any difference in behavior compared with the other specimens such as the 6 in. wide specimens, the results from the 3.5 in. wide single bolted connection can be directly compared with the results from the 6 in. wide double bolted specimens without any modification. For the specimens used in the test program, the interaction between net section stress and bearing stress is not a concern.

Effect of Buckling at Free End

Unexpected behavior was observed during the test of specimen AW450. The strength of the specimen dropped rapidly when the free end of the specimen buckled as shown in Figure 3-3. The buckling was caused by the lack of the lateral confinement. Moreover, the specimen slid a little along the bolt grip just before the buckling occurred. This was due to the initial crookedness of the specimen.

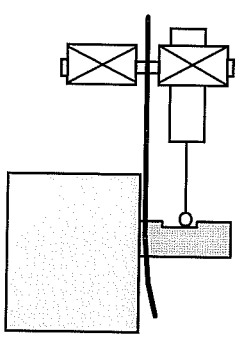

Figure 3-3 End Buckling

An attempt to restrain sliding of the specimen along the bolt grip was made first. A small clamping device was fabricated as previously shown in Figure 2-9. To minimize the friction, only a small area of the device was in contact with the specimen. With the clamping device, specimen AW45R was tested. The specimen buckled in the same way as specimen AW450, but the strength showed some increase.

Another attempt to eliminate the buckling at the free end was made. Instead of the small contact area through the plastic shim, full contact area was used by removing the plastic shim. It was assumed that there was not enough normal force to induce significant friction between the clamping device and the specimen because the clamping device was not completely fixed to the bolt grip. The build-up of material in front of the bolt hole could displace the clamping device along the bolt grip during the test. But, the device was installed firmly enough to restrain the sliding of the specimen and to provide some lateral confinement around the bolt hole. With this modification, specimen AW45S was tested and buckling did not occur. To confirm the behavior, specimen AW45U was tested as a replicate. AW45S and AW45U showed similar behavior.

As shown in Figure 3-4, the strength increased where lateral restraint was applied. The buckling occurred before the hole elongated 1/4 in. for specimen AW450. Actual strength at 1/4 in. displacement was used instead of the maximum strength for this plot even though the maximum strength was reached before the hole elongated 1/4 inches. The buckling of the free end would have had more effect on the strength if a larger clear end distance was used. If the specimens have had more thickness, buckling would not have been a problem. The effect of the buckling in free end is in good agreement with the previous report by Frank and Yura.

It can also be thought that the buckling in the free end of the specimen AW450 and AW45R is related to the net section stress. As the yielded portion of the net section increases, only small portion of the net section is effective in restraining buckling. For the other specimens including AW300, restraint was provided by the clamping device. Therefore, the buckling in the free end was not a concern.

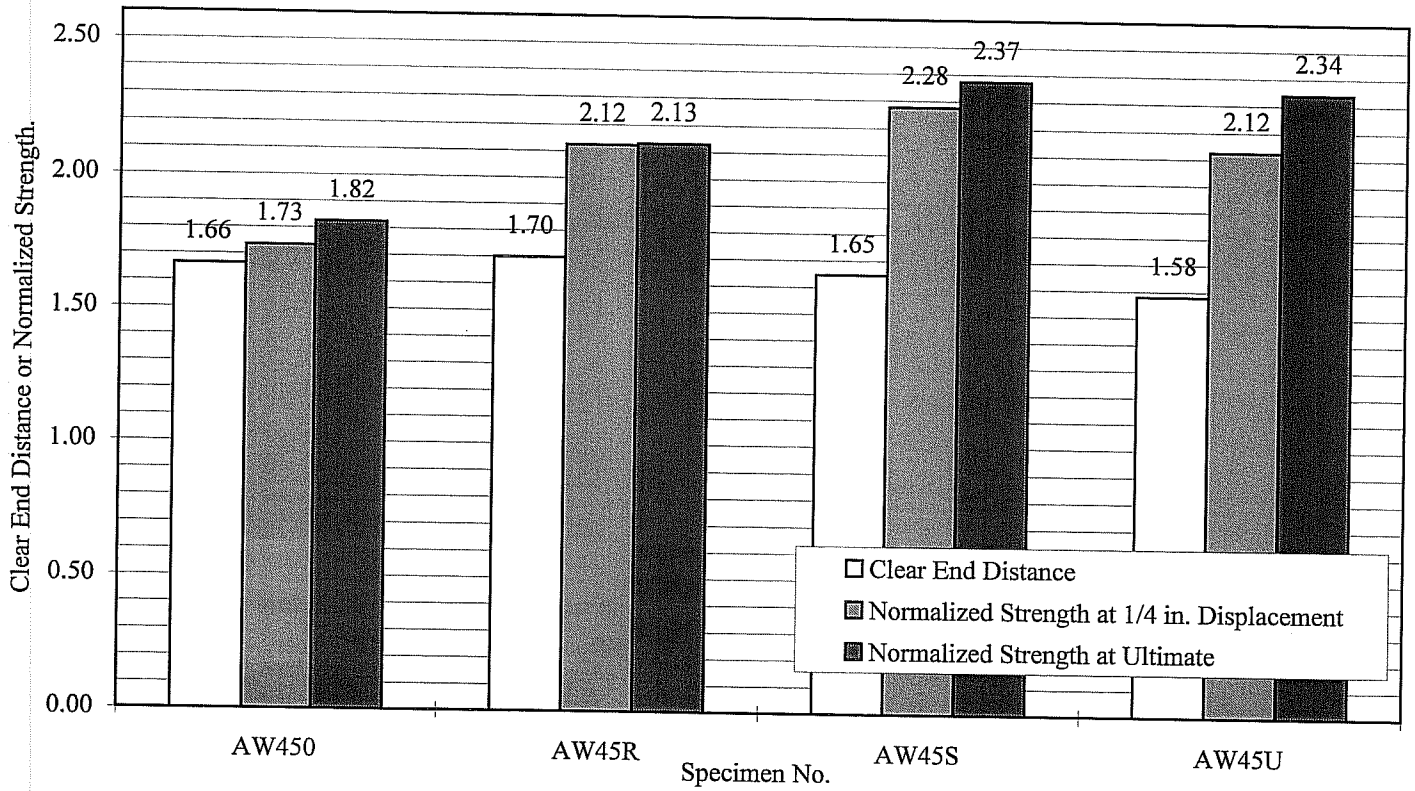

Figure 3-4 Effect of Lateral Confinement

3.1.2 AO, BO, AT, and BT Test Series

Effect of Yield Stress of Material

The strengths at 1/4 in displacement of each specimen were normalized with dtF_y and are plotted with respect to the clear distances normalized with d in Figure 3-5. For the double bolted connections, the average values of the clear end distance and clear spacing were used so that the double bolted specimens could be compared with the single bolted specimens. The normalized strengths of the specimens made of material A fall above the strengths of the specimens made of material B. The strengths at ultimate are plotted in Figure 3-6. Both the strengths at 1/4 in. displacement and the strengths at ultimate show a lot of scatter when normalized with the yield stress.

Effect of Ultimate Stress of Material

In Figure 3-7 and Figure 3-8, the strengths at 1/4 in. displacement and the strengths at ultimate are normalized with dtF_u. The normalized strengths of the specimens made of material A coincide with the normalized strengths of the specimens made of material B at various points. The plots show much less scatter compared with those which were normalized with dtF_y. Especially for the single bolted specimens with short clear end distance, little difference was noticeable between the strengths of the AO and BO test specimens. Therefore, it can be concluded that the strength at 1/4 in. displacement as well as the maximum strength is proportional to the ultimate stress rather than to the yield stress of the material.

3.2 Observations

AW Test Series

The failure mode for the AW test series was fracture at the edge of the hole. Yield lines could not be clearly seen. The yielded area spread from the area near the hole to the end. All of the specimens failed in shear fracture except for those that failed by buckling. Fracture due to shear stress is considered to be the conventional failure mode of bearing type connections. Fracutred specimen is shown in Photo 2.

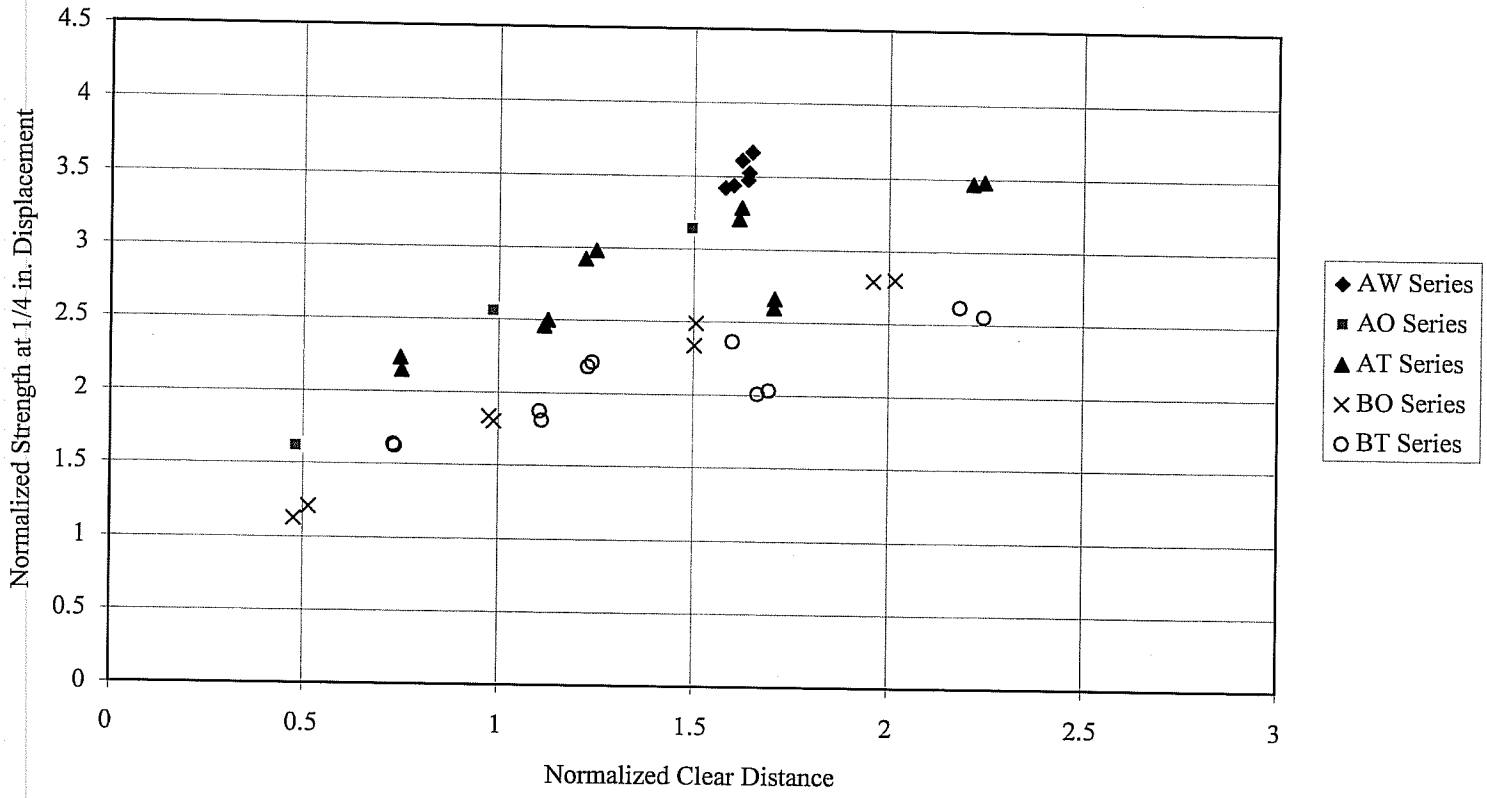

Figure 3-5 Strength Normalized by Yield Stress(1/4 in. Disp.)

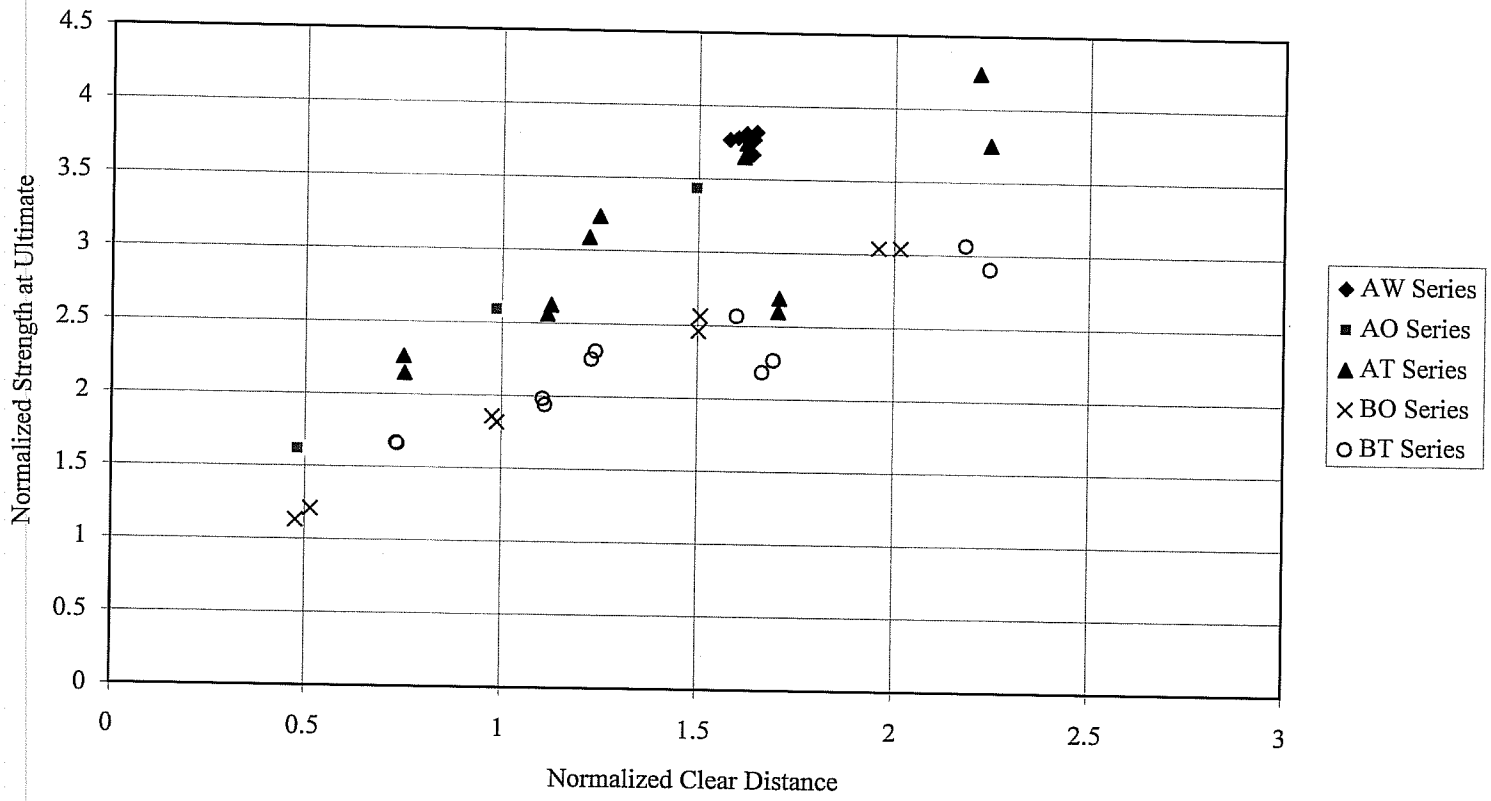

Figure 3-6 Strength Normalized by Yield Stress(at Ultimate)

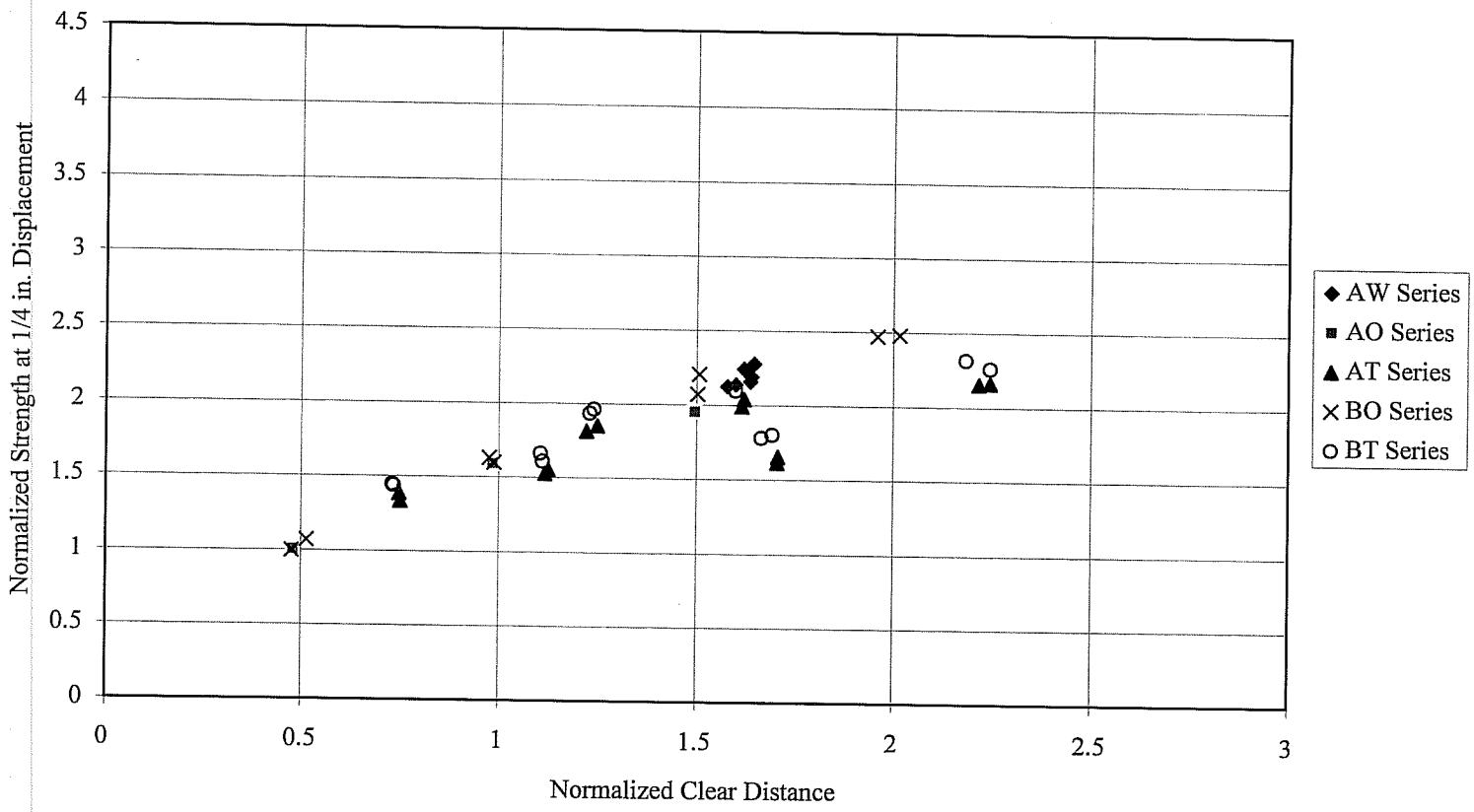

Figure 3-7 Strength Normalized by Ultimate Stress(1/4 in. Disp.)

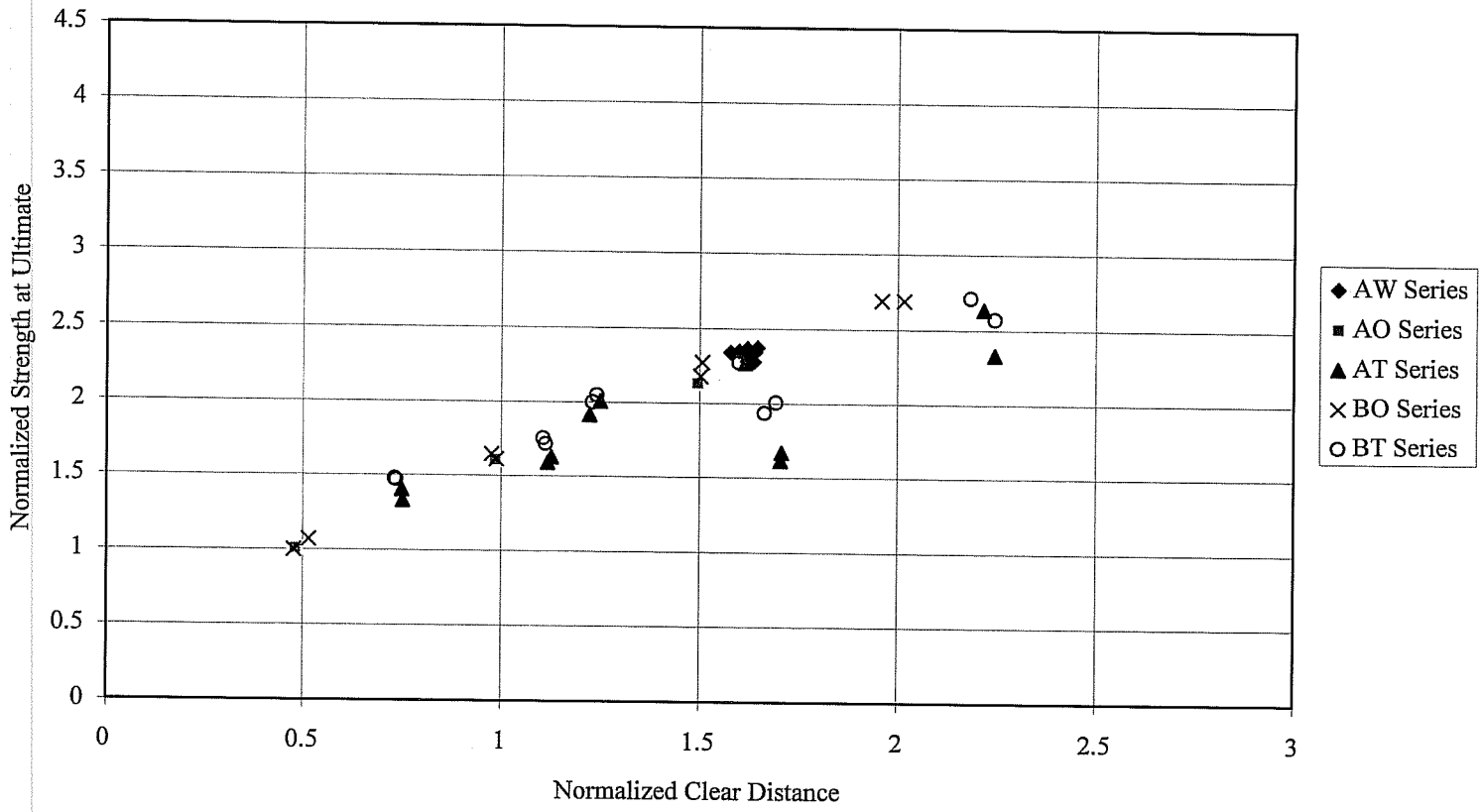

Figure 3-8 Strength Normalized by Ultimate Stress(at Ultimate)

AO Test Series

The failure mode was shear fracture around the edge of the hole. This is same as the failure mode in AW test series. Fractured specimens are shown in Photo 3 and in Photo 4. As the end distance increased, the shear fracture line got a little more inclined. The specimen AO100 shown in Photo 4 has a little more inclined failure line than the specimen AO050 shown in Photo 3. This could be due to the slight difference in stress distribution at the end.

For specimen AO200 and AO200R, the buckling limited the strength as shown in Photo 5. The area where the lateral clamping force was applied was not enough to restrain the buckling of the specimen.

BO Test Series

As shown in Figure 3-9, which compares the load-displacement curves of specimen AO100 and specimen BO100 with similar end distances, BO specimen showed a little more ductile behavior than AO specimen when the end distance is short. It was expected before the test that the specimens made of material A would be more ductile than the specimens made of material B since material A showed clearly more ductile behavior than the material B in the coupon test. It has been usually thought that structures made of the material with high ultimate stress to yield stress ratio tends to have ductile behavior. Test results are not in accordance with this conventional measure of the ductility.

As the end distance increased, the deformation at failure increased as shown in Figure 3-10. Ductility of the connection seemed to be influenced by the end distance when the end distance is short. Therefore, more ductile behavior can be achieved by avoiding short end distance as long as the buckling in the free end is prohibited.

When ductility is compared at the same strength level as shown in Figure 3-11, specimens made of material A shows more ductile behavior than the specimens made of material B. Therefore, the end distance is a more influencing factor on ductility than the material property when the end tearout failure mode is concerned.

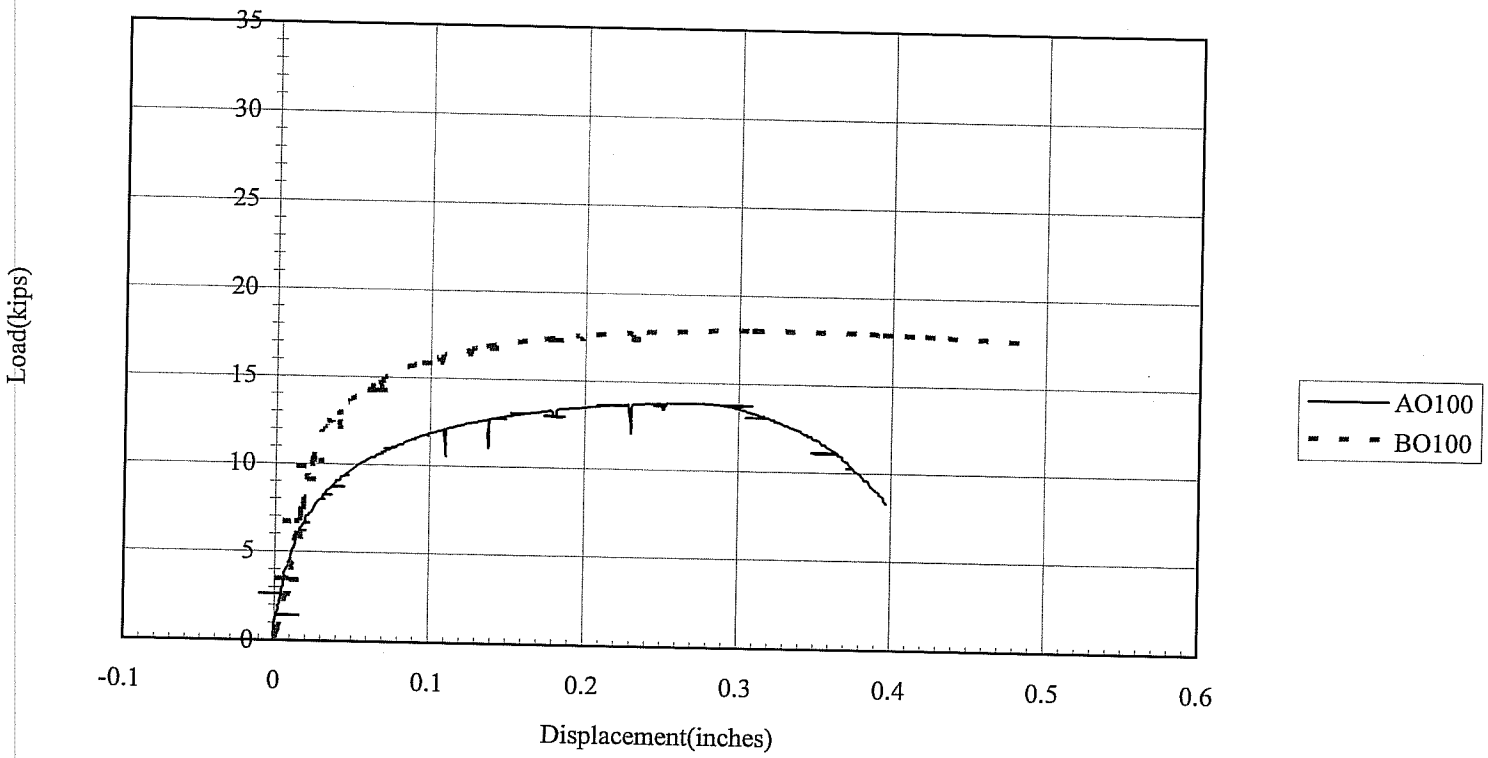

Figure 3-9 Comparison of Ductility

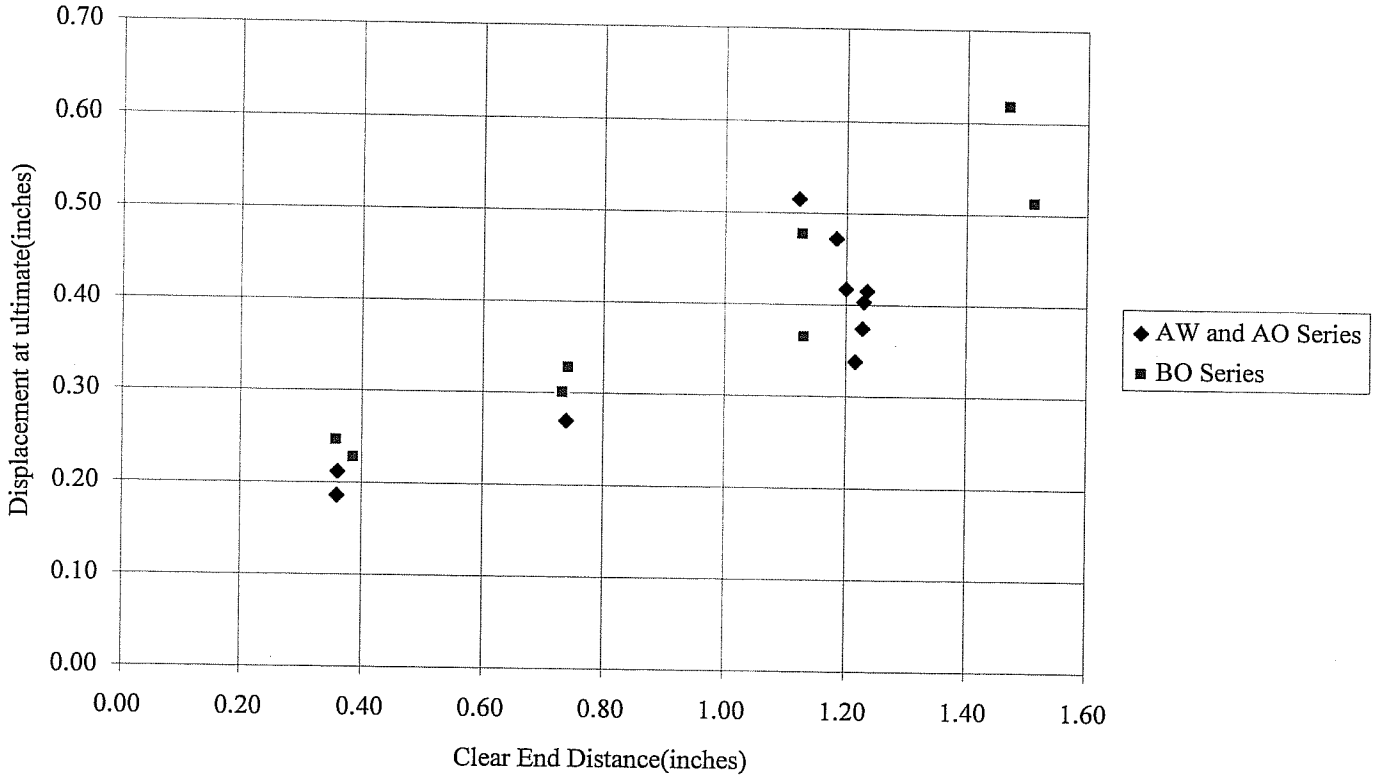

Figure 3-10 Effect of End Distance on Deformation Capacity

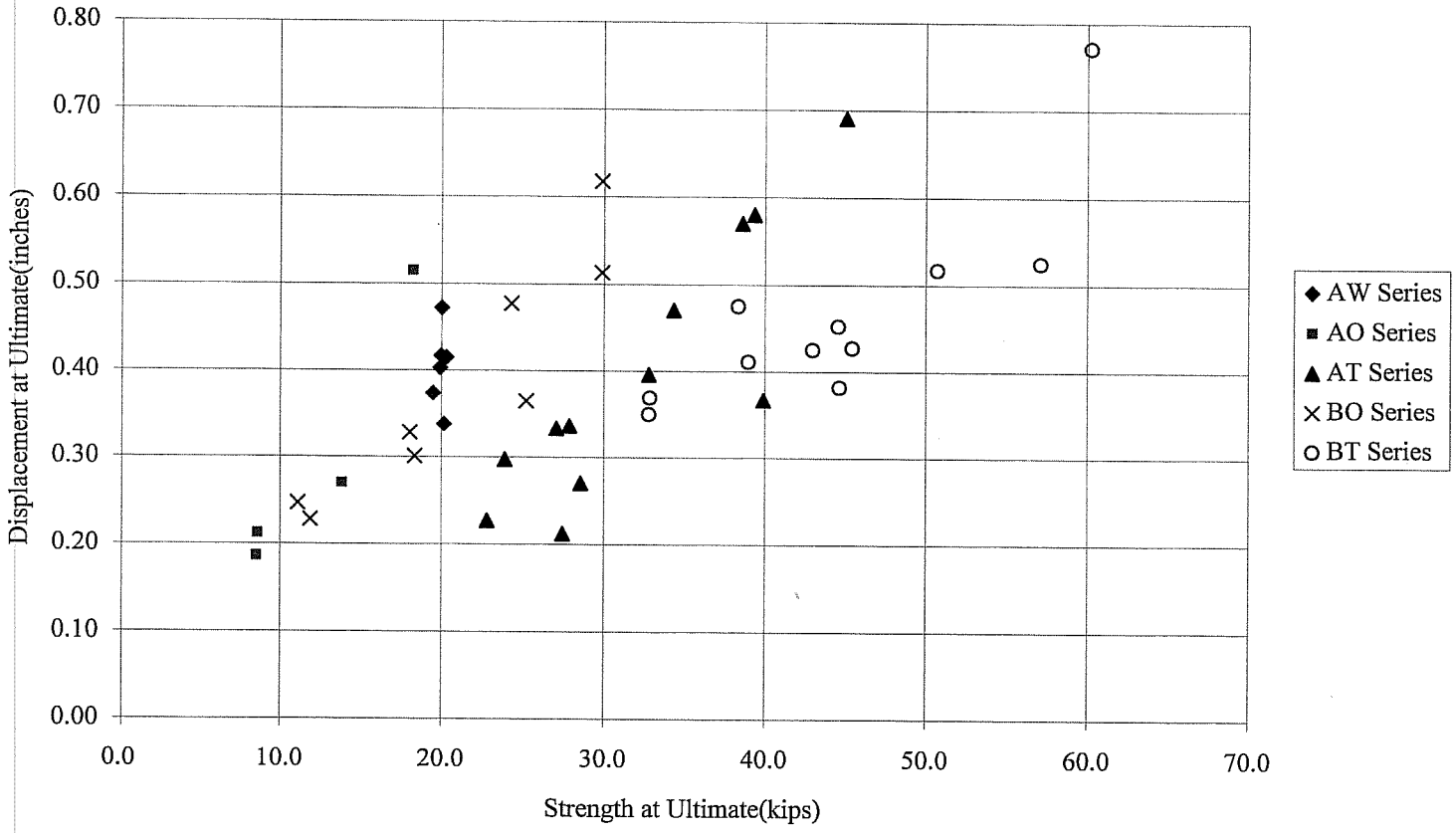

Figure 3-11 Deformation Capacity

Contrary to the specimens in the AW and AO test series, the specimens in the BO test series showed clear yield lines. The yield lines shown in Photo 8 clearly defines the principal stress path which originates from the edge of the hole and propagates to the end of the specimen. The ultimate strengths of specimen BO150 and specimen BO150R were limited by the initiation of fracture at the end. For the other specimens in BO test series, shear fracture at the edge of the hole limited the ultimate strength, which is the same the failure mode as in the AO and AW test series. Specimen BO150 and the specimen BO150R differed from the other specimens in that they had sheared ends. The coarse end was susceptible to stress concentrations and reduced ductility due to shearing. The fracture at the end occurred at the place where the two yield lines met.

The photos associated with the load-displacement curves in Figure 3-12 were presented in Photo 6, 7, 8, 9, 10, and 11. The specimen assembled in the fixture is shown in Photo 6. The clamping device mounted on the bolt can be seen. When the specimen is loaded, the yielding starts from the edge of the hole where the bolt bears. The yield area in front of the bolt is shown in Photo 7. The yielded area increases as the load increased. At the low loading, the yielded area was restricted to the area in front of the bolt. As the load increased more, the yielded area spreads toward the side edge of the specimen and toward the end of the specimen. The yield lines develop from the edge of the hole and advances toward the end of the specimen as shown in Photo 8. The yield lines are narrow at the beginning. This yield lines get thicker and short yield lines perpendicular to the principal yield lines form. This is shown in Photo 9. This short yield lines indicate the direction of the tensil stress. The material in the area enclosed by the yield lines get yielded as the load increased more. As the material yields, the deformation of the hole gets significant. Finally, the material from the hole to the end yields completely and the fracture develops as shown in Photo 10 and Photo 11.

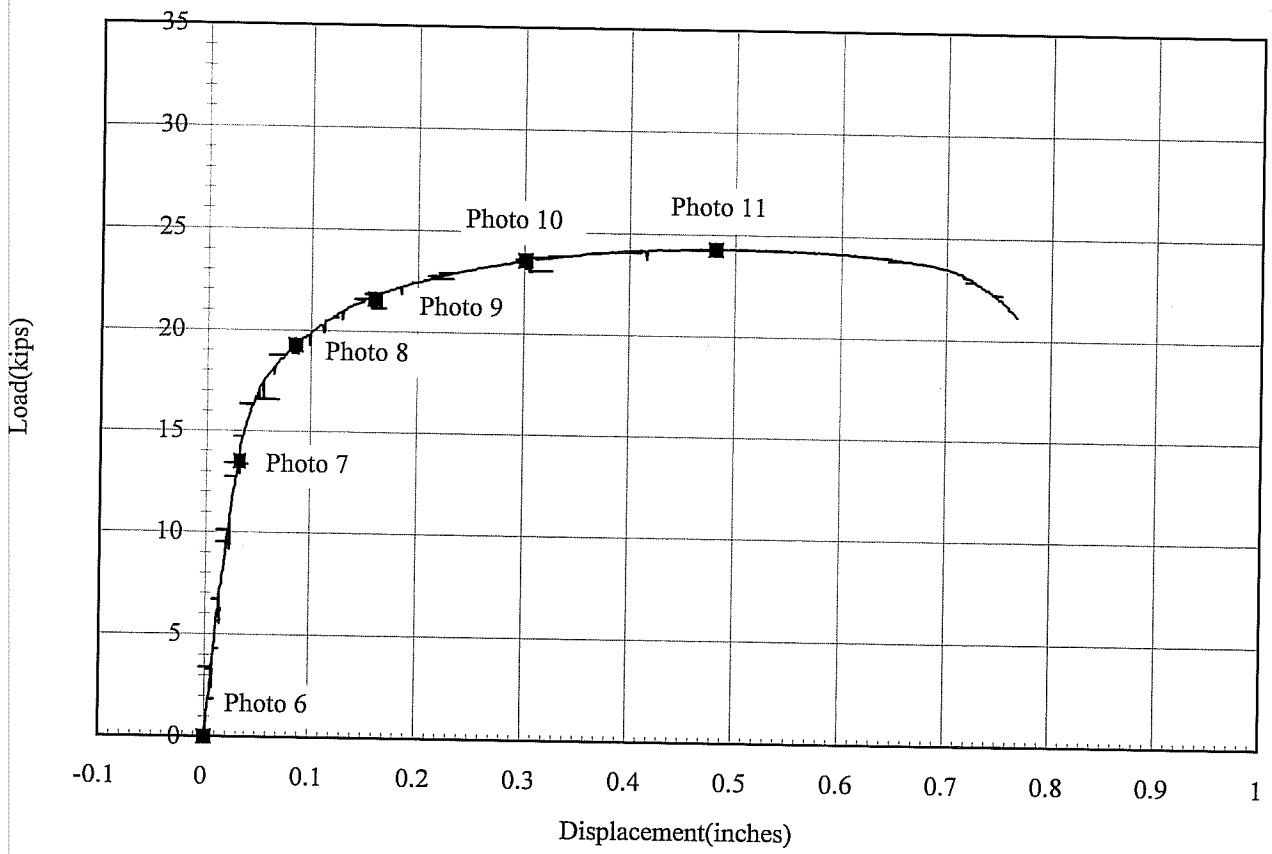

Figure 3-12 Load-Displacement Curve of Specimen BO150

AT Test Series

In the AW, AO, and BO test series, the fracture started from the end for the specimens that had a sheared end and it started from the edge of the hole for the other specimens. Therefore, it was expected that the fracture at the edge of the hole would occur for specimens with a sawed end in the AT test series. For most of the specimens with the short clear end distance of 0.5d, the maximum strength was reached when the fracture occurred at the edge of the first bolt hole. But, a fracture at the end limited the strength for most of the specimens with a clear end distance of 1.5d in the AT test series even though their ends were not sheared. Only specimen AT0530 and AT1530 had sheared ends. For specimen AT1530, fracture started from the end. It is not clear whether the fracture in the specimen AT0530 started from the end or not.

Since some specimens without a sheared end show an end fracture, the fracture at the end can be attributed not only to the coarse end condition of the sheared specimen but also to some other factors for the sawed specimen. It is considered that the specimens with a 1.5d clear end distance fractured at a large displacement compared with the specimens with a 0.5d clear end distance. As mentioned before, specimens with longer end distances have more deformation capability. The edge of the hole of the specimen with a 1.5d end distance could undergo large deformation without developing any fracture. In this case, the end gets thin which becomes vulnerable to fracture before the fracture initiates at the edge of the hole at large displacement. For specimens with a short end distance, the fracture at edge of the hole initiated before the end gets thin.

A particular failure mode was noted for most of AT test series. As shown in Photo 12 of specimen AT0530, yield lines similar to those in the BO test series form in front of the second hole. The stress concentration on top of the first hole can be clearly seen. The failed end due to the fracture around the first hole separates which induces more tensile stress on the top of the first hole. This leads to the tensile fracture at the top of first hole as shown in Photo 13.

When the spacing is short, a fracture at the top of the first hole or a fracture at the edge of the second hole limited the strength. As shown in Photo 14 and Photo 15 of

specimen AT1510, a fracture started on the top of the second hole before a fracture started at the end. For specimen AT1510R, a fracture at the edge of the second bolt limited the strength.

As shown in the Tables 3-2 and 3-3, the two-bolt specimens with a short end distance can not reach the full strength that is estimated by the sum of strengths of each bolt hole. The strength difference between specimen AT1510 and specimen AT0510 should be same as the difference between specimen AT1530 and specimen AT0530 since the difference between the end distances for each pair of tests is the same. But, as shown in the table, specimen AT0530 has much less strength than AT1530. The short end failed before the second bolt reached its maximum strength for specimen AT0530. The strength dropped when the end failed due to fracture.

BT Test Series

Specimens with a 1.5d end distance failed in fracture at the end while those with a 0.5d end distance failed by fracture at the edge of the first hole. This is the same behavior as noted in the AT test series.

Yield lines between the two holes in specimen BT0530 can be seen in Photo 16. The shape of the yield lines is same as those in the BO test series. The stress concentration on the top portion of the first hole and on the side of the edge of the second bolt would cause the fracture. Since the end distance is short compared with the spacing, the short end failed first and limited the strength.

The build-up of material in front of the second bolt increased the thickness. The force transferred to the second bolt increased due to the thickness increase. The thickness increase was not considered in the calculation of the size of the bolt to resist the shear force. The increased thickness of the material due to the build-up caused the bolt to bend as shown in Photo 17. Since the end failed before the bolt bent, the error in the deformation measurement was not a concern.

Table 3-2 Effect of Short End Distance(AT Series)

	AT1510 and AT1510R	AT0510 and AT0510R	Difference
Strength at 1/4 in.	31.3 kips	23.2 kips	8.1 kips
Strength at Ultimate	33.6 kips	23.4 kips	10.2 kips

	AT1520 and AT1520R	AT0520 and AT0520R	Difference
Strength at 1/4 in.	34.2 kips	26.3 kips	7.9 kips
Strength at Ultimate	39.0 kips	27.5 kips	11.5 kips

	AT1530 and AT1530R	AT0530 and AT0530R	Difference
Strength at 1/4 in.	37.0 kips	27.9 kips	9.1 kips
Strength at Ultimate	42.5 kips	28.1 kips	14.4 kips

Table 3-3 Effect of Short End Distance(BT Series)

	BT1510 and BT1510R	BT0510 and BT0510R	Difference
Strength at 1/4 in.	43.3 kips	32.1 kips	11.2 kips
Strength at Ultimate	45.0 kips	32.9 kips	12.1 kips

	BT1520	BT0520 and BT0520R	Difference
Strength at 1/4 in.	46.8 kips	36.4 kips	10.4 kips
Strength at Ultimate	50.7 kips	38.7 kips	12.0 kips

	BT1530 and BT1530R	BT0530 and BT0530R	Difference
Strength at 1/4 in.	50.8 kips	39.8 kips	11.0 kips
Strength at Ultimate	58.7 kips	43.8 kips	14.9 kips

3.3 Failure Mode

The failure mode is associated with the following behavior

1. Build-up of material in front of the bolt.
2. Yielding around the hole.
3. Yielding at the edges of the connected member.
4. Width increase at the end of the specimen.
5. Fracture either at the end of the connected member or at the edge of the hole.

The conventional failure line for the end tearout failure mode is the inclined straight line from the edge of the hole to the end of the specimen as in Figure 3-13. The failure lines for test specimens made of material A follow this line. But, the actual failure line associated with the maximum strength is thought to be the curved lines which are same as the yield lines in Figure 3-14. The fracture at the edge of the hole changes the geometric configuration and accordingly the stress distribution. The curved failure line seems to change into a straight line after fracture starts. The strength drops when the fracture starts before the conventional failure lines form. The conventional failure lines are not the failure lines associated with the maximum strength.

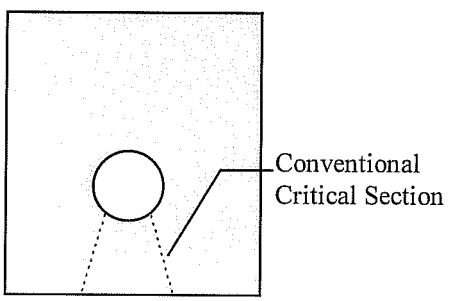

Figure 3-13 Critical Section

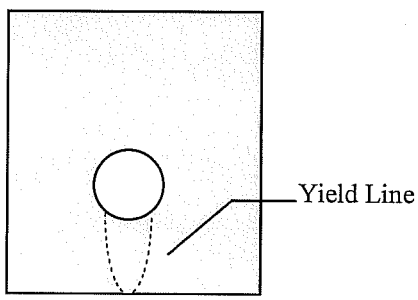

Figure 3-14 Yield Lines

A fracture at failure started either from the edge of the hole or at the end of the specimen on the yield lines for one-bolt connections. The fracutre at the edge of the hole is due to the shear stress. The fracture at the end is due to the transverse tensile stress.

As the specimen deforms, material at the end gets thinner and the fracture initiates. For the two-bolt connections with large end distance and short spacing, a fracture at either (a) or (b) in Figure 3-15 occured, and for the specimen with short end distance and long spacing, the fracture at either (c) or (d) limited the maximum strength. Fracutures initiated at (a) or (c) change the geometry as they developes. This results in a change in the stress distribution, and the the critical section defined by the yield line changes. As the fracture advances, it follows the lines defined by the conventional failure section. This is not applicable to the fracture initiated from the end of the specimen. For a few specimens, the fracture formed at the end and followed the yield line as it developed. The failure line was the same as the lines defined by the yield lines. The fracture developed on either the left or the right half of the yield line. For other specimens, the fracture at the end advanced vertically upward. Especially for the two-bolt specimens, the crack which formed at (b) advanced vertically. This vertical fracture path between two holes was clearly noticeable. As the bolt advances through the yielded area, the bolt pushes the material sideward and downward, which results in a width increase at the end. As the bolt pushes the material sideward, the force separating the specimen into a left half and a right half developes. This increases the tensile stress at in the area where the fracture has formed. Therefore, the fracture advances vertically.

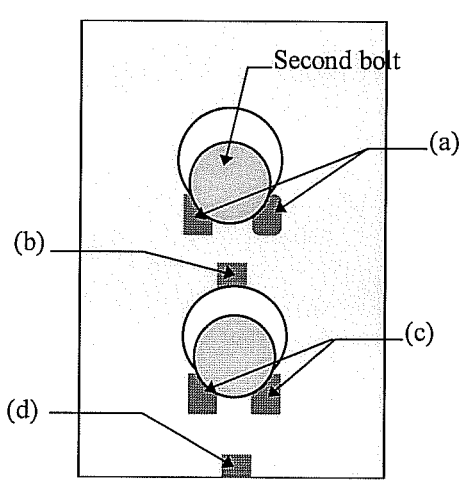

Figure 3-15 Fracture

Yielding of the material at the left and right edge of a specimen is shown in Figure 3-16. The yielding around the hole results from the stress concentration. The yielding at the sides is not considered to be due to the stress concentration. As the width at the end increases, the separating force as mentioned above also induces bending at the net secion. This bending stress seems to cause compressive stress along the outer edge of the specimen.

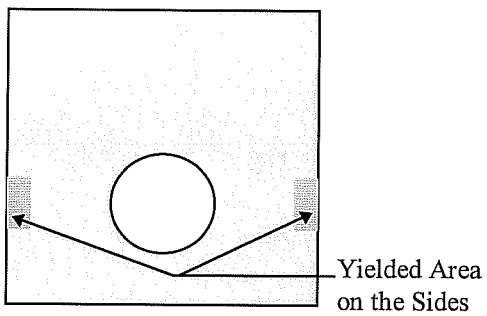

Figure 3-16 Yielding at the Edge of a Specimen

CHAPTER 4

Comparison with Design Equations

The test results of one and two-bolt connections are compared with the strengths at 1/4 in. displacement and at ultimate predicted by the design equations in AISC-LRFD and by the design equations in reference 12. And, the results of the one-bolt connections are compared with the ultimate strengths predicted by Winter[11], by Chong and Matlock[3], and by Kennedy and Sinclair[7]. The strength reduction factors were not used for the calculation of the strength predictions. The test results from Lewis[9] are compared with AISC-LRFD design equations.

4.1 Comparison with AISC-LRFD and Design Equations in Reference 12

The strength at 1/4 in. displacement was predicted by LRFD accurately as shown in Figure 4-1. For the single bolted specimens, the predictions are quite close to the test results. The predictions of strength for the two-bolt connections have a little more scatter compared with the predictions for one-bolt connections, but, they are still considered to be accurate enough.

When deformation around the bolt holes is not design consideration, LRFD has separate design equations. For the application of these equations, LRFD requires the end distance to be more than 1.5d and the spacing to be more than 3.0d. Only a few specimens met these requirements in the test program. Figure 4-2 shows the comparison of these test results with AISC-LRFD predictions.

Strength predictions at 1/4 in. displacement and at ultimate in a clear distance approach[12] are $1.2L_ctF_u \leq 2.4dtF_u$ and $1.5L_ctF_u \leq 3.0dtF_u$ respectively. Strength predictions at ultimate can be used only if there are two or more bolts in the line of force. In Figure 4-3, most of the test results at a 1/4 in. displacement fall on the conservative side. The equations based on the clear distance approach underestimate the strength at 1/4 in. displacements. But, as shown in Figure 4-4, the strength predictions at ultimate are as good as the strength predictions by LRFD.

In AISC-LRFD, $L_e tF_u$ for the bolt hole nearest the end and $2.4dtF_u$ for the remaining bolt holes are used when the end distance is not less than 1.5d and when the spacing is not less than 3.0d. Specimens such as AT1530 satisfy this requirement while specimens such as AT0530 do not meet the requirement since the end distance is less than 1.5d. For the specimens which do not satisfy the requirement, $L_e tF_u$ for the end bolt hole and $(s-d/2)tF_u$ for the remaining bolt holes should be used. When the spacing is not less than 3.0d, the strength predictions mentioned above are applicable from the spacing of 1.5d, which cause a sudden jump in the strength prediction as shown in Figure 4-5. The test results are compared with these predicted strengths in the figure. Since all the specimens shown in the figure have similar spacing, the contribution of the second bolt hole on the strength due to the end distance of 3.5d is subtracted from the measured strength. As shown in the figure, the test results fall on the dotted line which is the extension of the solid line based on $L_e tF_u$ and $(s-d/2)tF_u$. The discontinuity at the end distance of 1.5d in AISC-LRFD is not confirmed by the test results.

4.2 Comparison with Other Strength Predictions

Figure 4-6 shows a comparison of the test results with the strength predictions in Reference 8. Data point of (1) in the figure is based on the strength predictions using the clear end distance and data points of (2) is based on the predictions using the centerline dimension. Strength predictions are $1.4(C1)tF_u$ and $L_e tF_u$ respectively. Both of these equations use ultimate stress of the plate. When the strength is low, which means a short end distance, the prediction based on the centerline dimensions is quite accurate and the predictions based on the clear distance is a little conservative. As the end distance gets large, the predictions based on the clear distance gets closer to the test results. These are in agreement with the study in Reference 8.

In Figure 4-7, strength predictions by Winter, by Chong and Matlock, and by Kennedy and Sinclair are compared with the test results. Their predictions are $1.4L_e tF_y$, $1.08L_e tF_y$, and $(1.257L_e+.174)\ tF_y$ respectively. Data points of (1), (2), and (3) represents their predictions. These predictions are based on yield stress and have more scatter than

the predictions mentioned previously. Two outer lines bound 80% and 120% of the predicted loads. The predictions by Winter fall within these lines, as is mentioned in Reference 11.

The test results from Lewis[9] are also compared with AISC-LRFD design equations in Figure 4-8. Strengths of one-bolt connections show good agreement with the predictions. Compared with the test data in Figure 4-1, data in Figure 4-8 resulted from the tests with thicker steel plates.

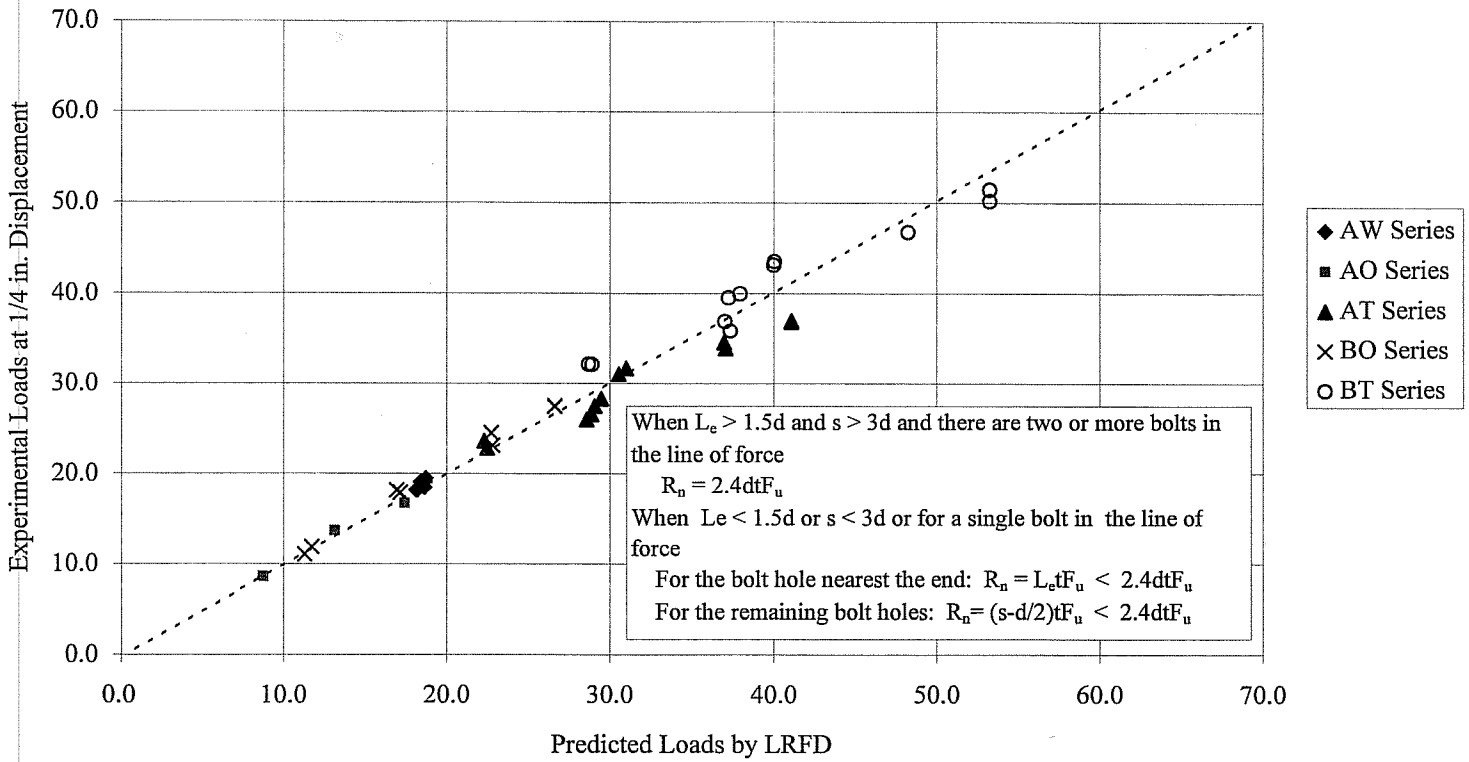

Figure 4-1 Comparison with AISC-LRFD(1/4 in. Disp.)

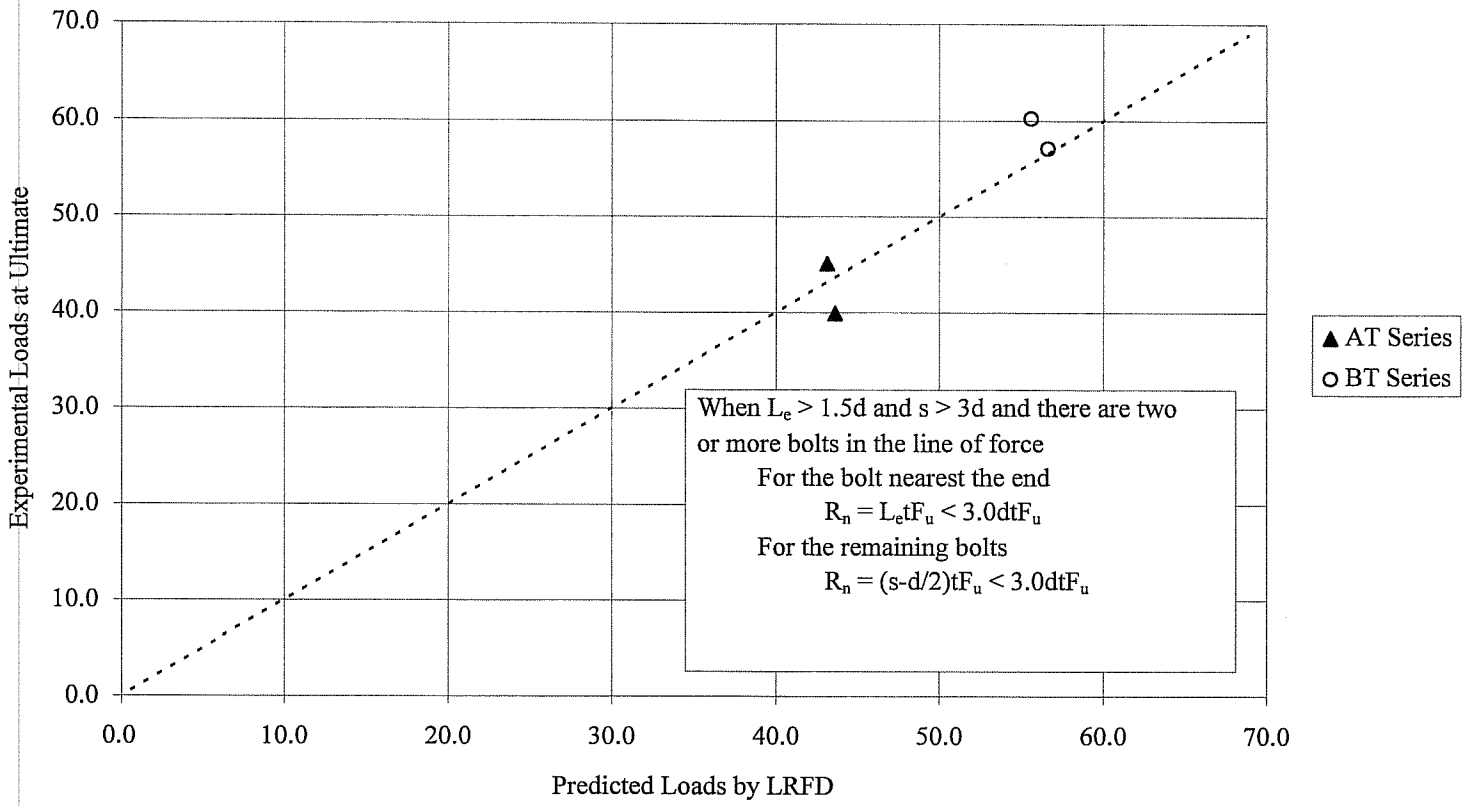

Figure 4-2 Comparison with AISC-LRFD(at Ultimate)

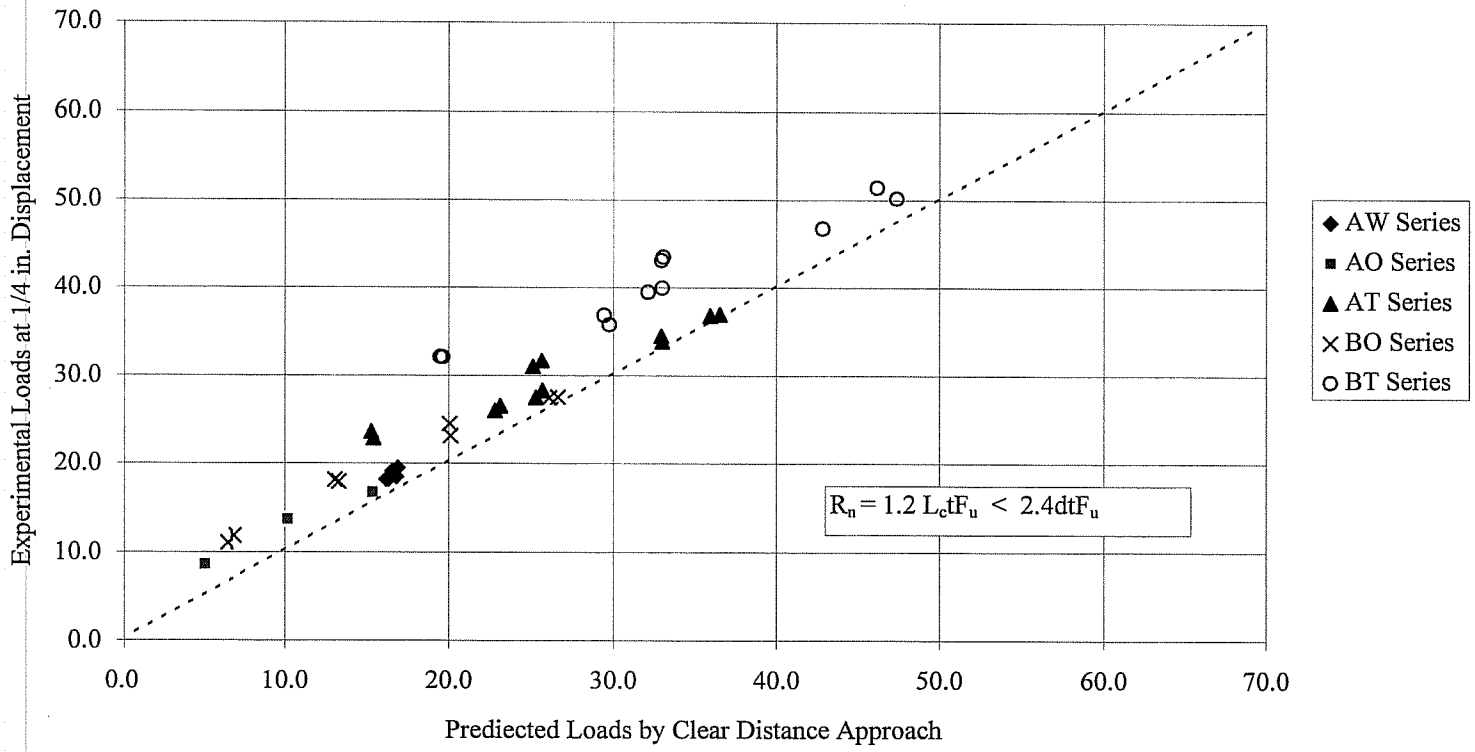

Figure 4-3 Comparison with Clear Distance Approach(1/4 in. Disp.)

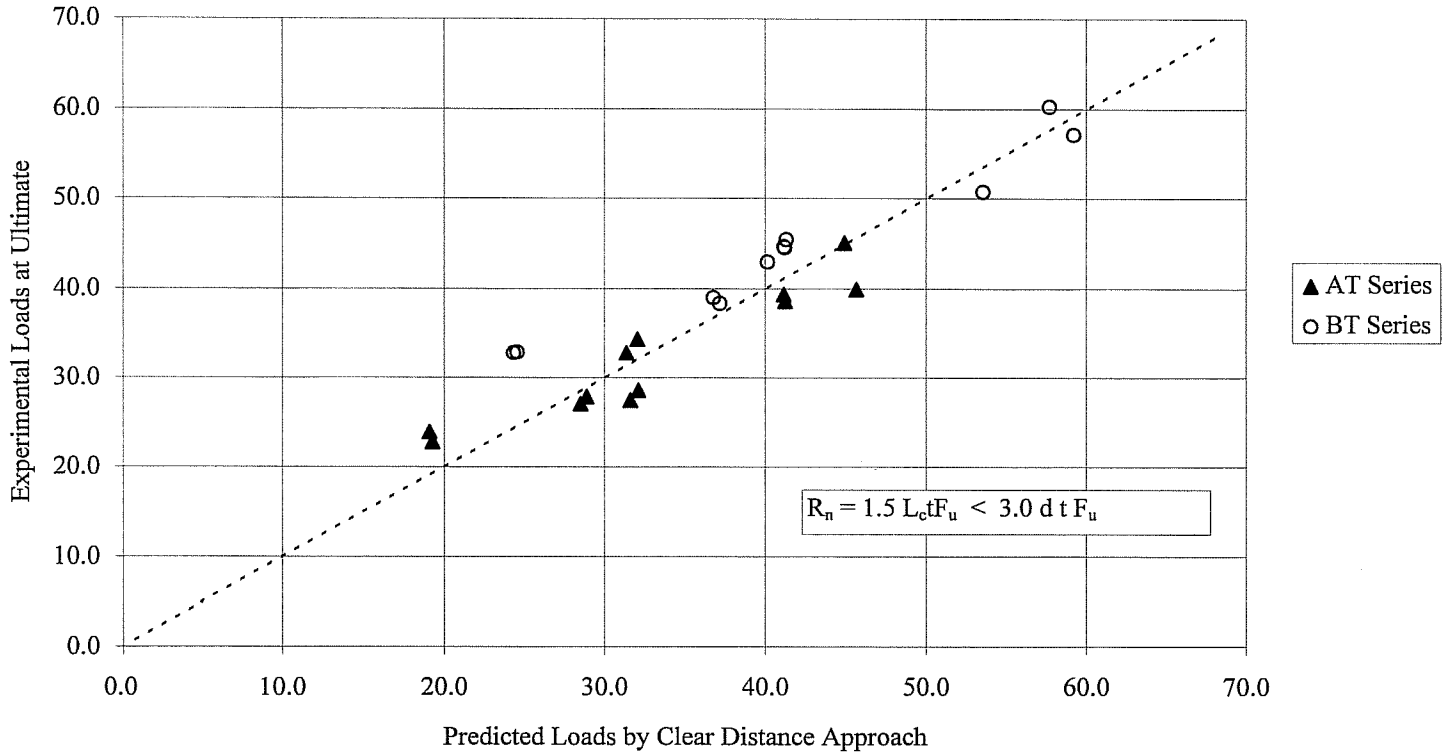

Figure 4-4 Comparison with Clear Clear Distance Approach(at Ultimate)

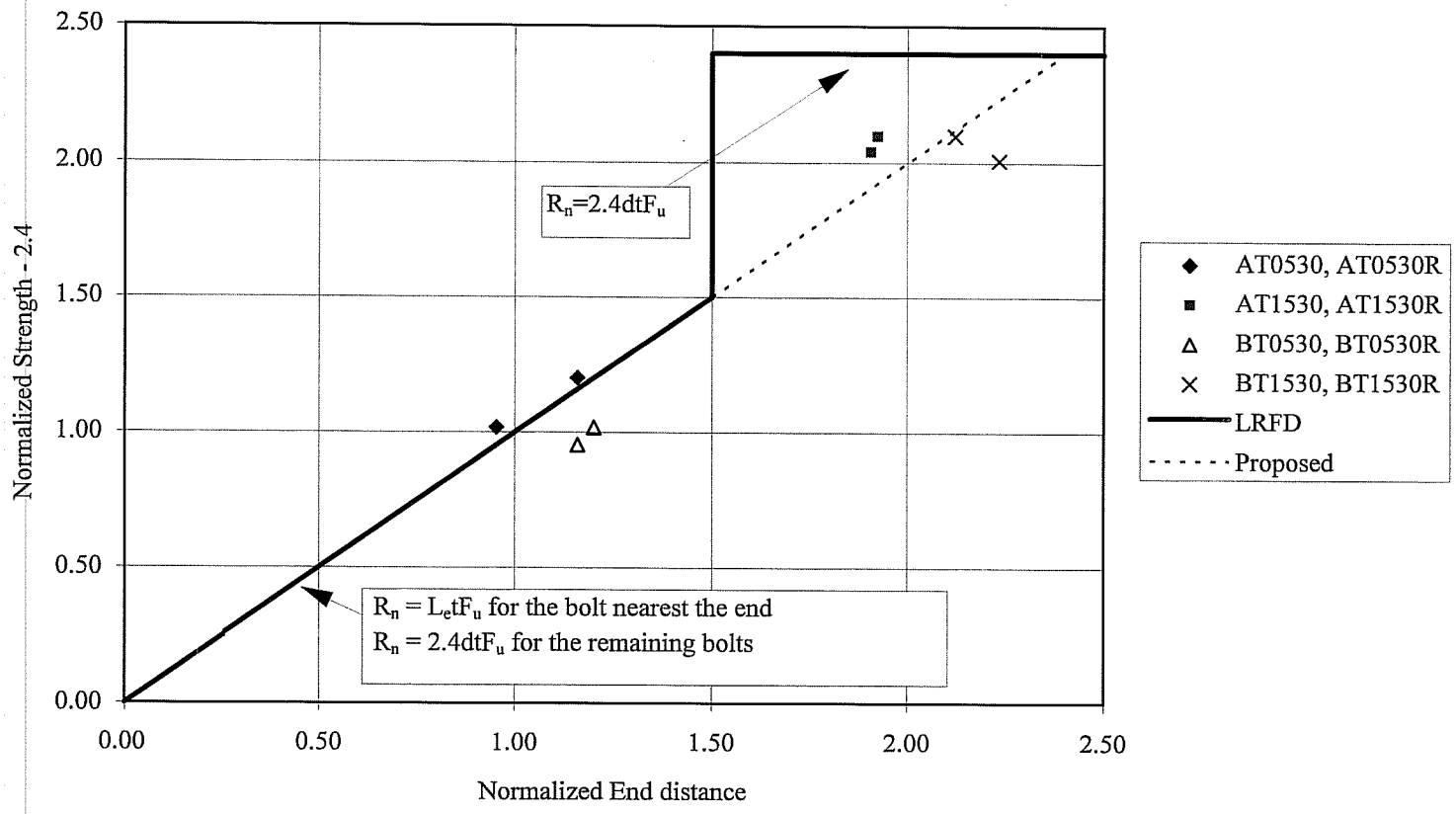

Figure 4-5 Comparison with AISC-LRFD(Spacing > 3.0d)

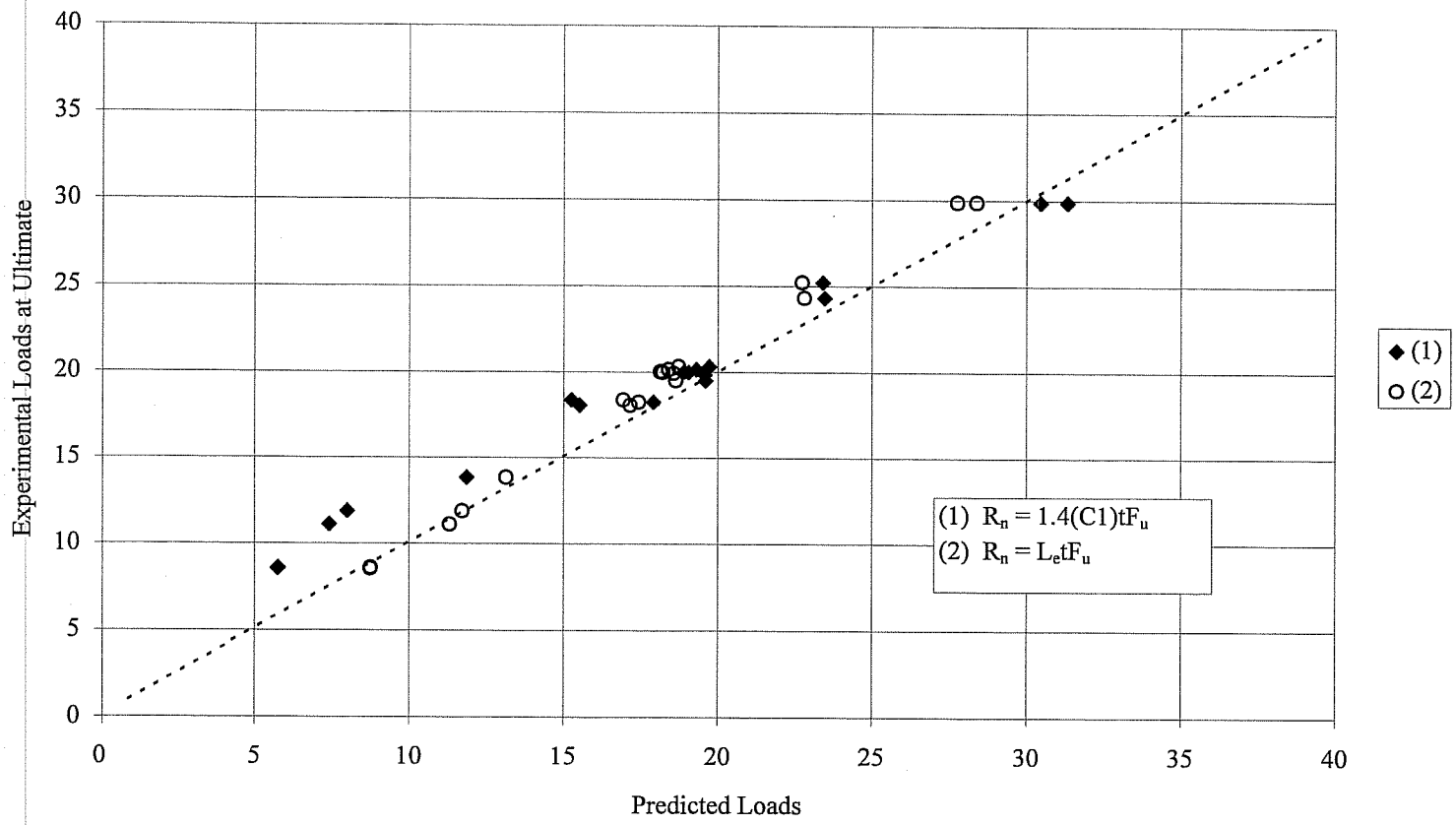

Figure 4-6 Comparison with Design Equations(Ref. 8)

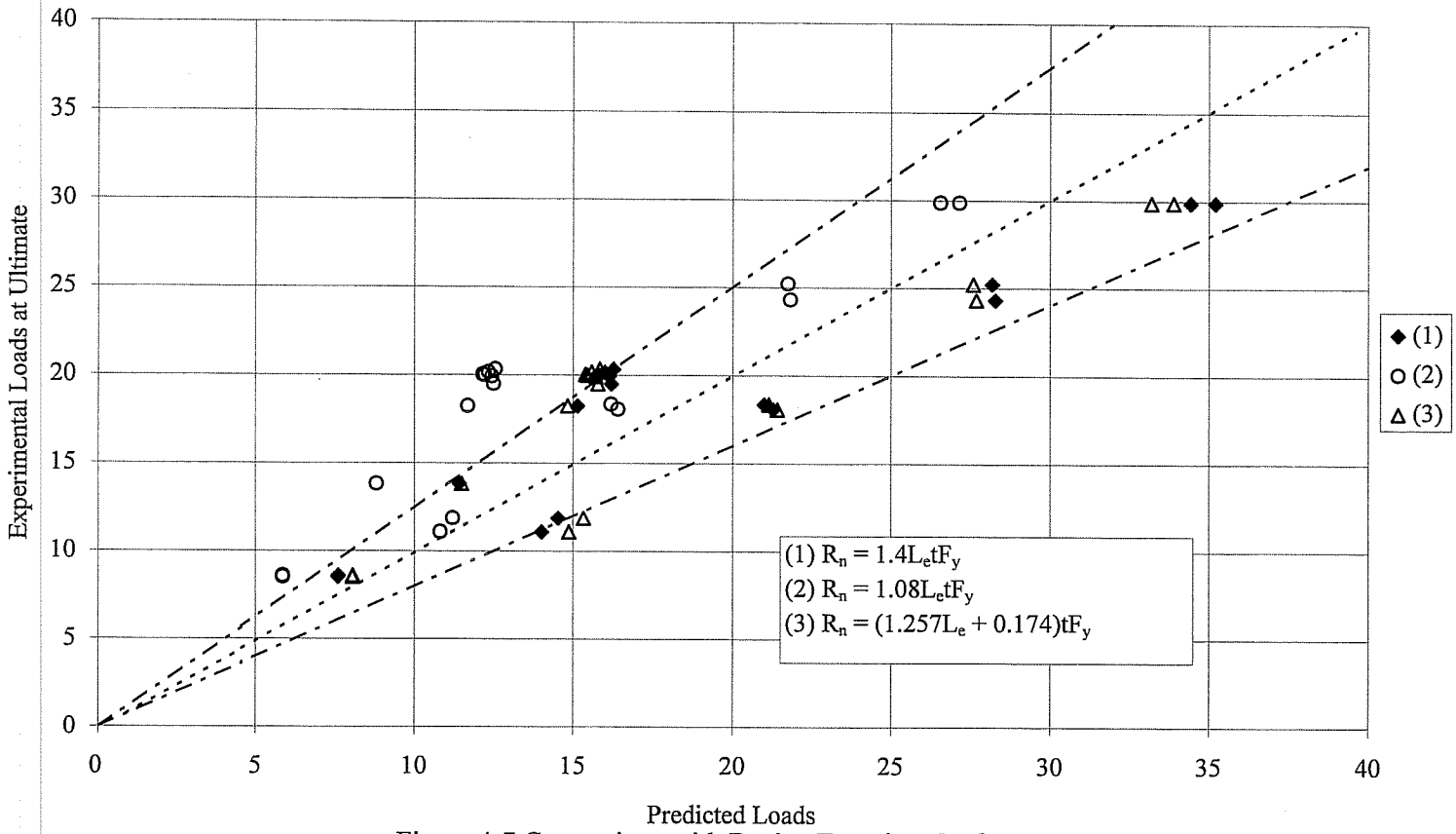

Figure 4-7 Comparison with Design Equations(Ref. 11, 3, 7)

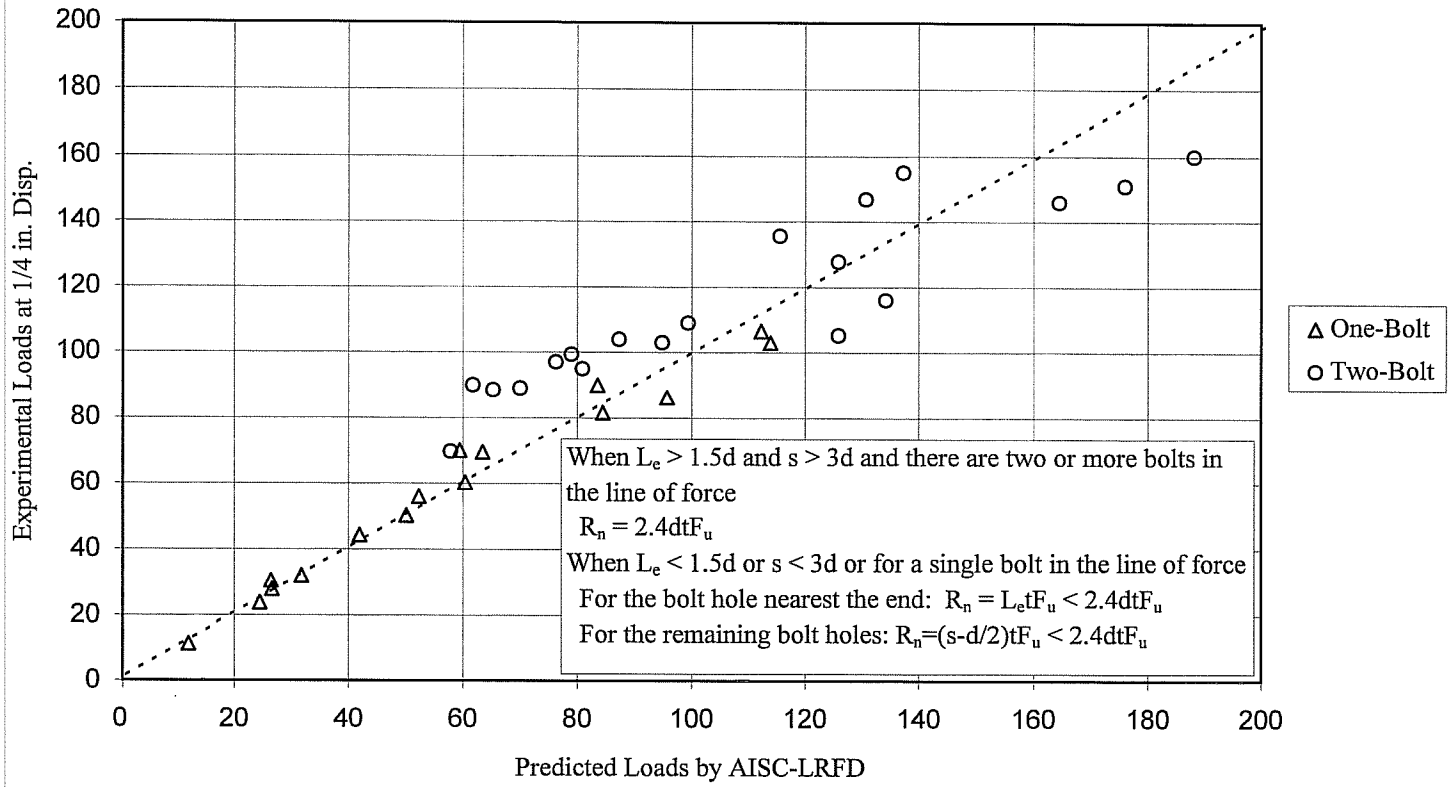

Figure 4-8 Comparison of the Test Results by Lewis[9] with AISC-LRFD

CHAPTER 5

Conclusions

In the test program, the frictional force was removed by eliminating the nuts on the bolts, and the bolts were placed mostly in punched holes. It was reported by Ibrahim[13] that the shear strengths of hand tight bolts placed in punched holes were lower than the shear strength of hand tight bolts placed in drilled holes by 13%. Therefore, the strengths at 1/4 in. displacement and at ultimate in the test program gave lower limits of the strength for the end tearout and the bearing failure modes. On the other hand, the use of dynamic shear strengths of each specimen instead of static strengths would result in higher strengths. The dynamic strengths were about 4% higher than the static strengths and the differences were disregarded.

1. The ultimate to yield stress ratio does not affect the strength at 1/4 in. displacement, and the bearing strength associated with the end tearout failure mode is proportional to the ultimate stress.
2. Ductility is affected by the end distance when the distance is short.
3. The conventional AISC-LRFD design equations give strength predictions close to the test result for single bolted connections. The clear distance approach is conservative for the connections with a short clear end distance because of the reserve strength at a zero clear distance.
4. For the double bolted connections with short end distance and large spacing, the short end distance limits the strength. If the end distance is short, there should be a limit on the spacing to be considered effective for the strength prediction.
5. The discontinuity at the end distance of 1.5d in AISC-LRFD is not confirmed by the test result.

APPENDIX

Test Specimen Data

Exemplary calculations are shown and test data are presented.

Data Processing

As an example, geometric configurations of specimen BO200 are shown in Figure A and data readings and calculated values are listed in Table A.

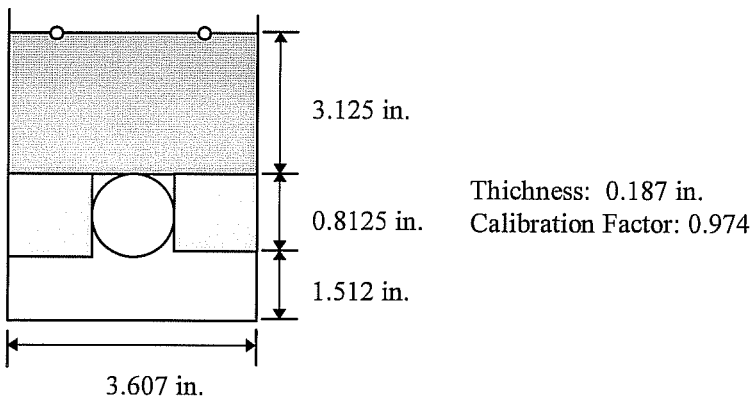

Figure A

Table A

Data Readings		Calculated Values	
Load (volt)	Displacement (volt)	Displacement (inch)	Load (kips)
0.0	**2.724**	**0.0**	**0.0**
-	-	-	-
3.933	**3.901**	**0.223**	**26.527**

1. Load

(Reading - Initial Reading) • (Conversion Factors)

(**3.933** volt - **0.0** volt) • (300 KN. / 10 volt) • (1 kips / 4.448 KN.) = **26.527** kips

2. Displacement

A. Total Displacement

(Reading - Initial Reading)•(Conversion Factor)•(Calibration Factor)

(**3.901**volt - **2.725** volt) • (2 in. / 10 volt) • (0.974) = 0.229 in.

B. Elastic Deformation in Gross Section

(Load • Length) / (Elastic Modulus • Width • Thickness)

(**26.572** • 3.125) / (29000 • 3.607 • 0.187) = 0.004 in.

C. Elastic Deformation in Net section

(Load • Length) / (Elastic Modulus • Width • Thickness)

(**26.572** • 0.8125) / (29000 • (3.607 - 0.8125) • (0.187) = 0.002 in.

Therefore, Deformation = 0.229 - 0.004 - 0.002 = **0.223** in.

Test Data

Load-displacement curves are plotted after input data readings of each specimen are processed. The graphs of load-displacement curves are presented in Figure B. Replicates are plotted as dashed lines in the graphs. Spikes in the graphs are due to a temporary surge of the voltage, which would not affect the accuracy of the results.

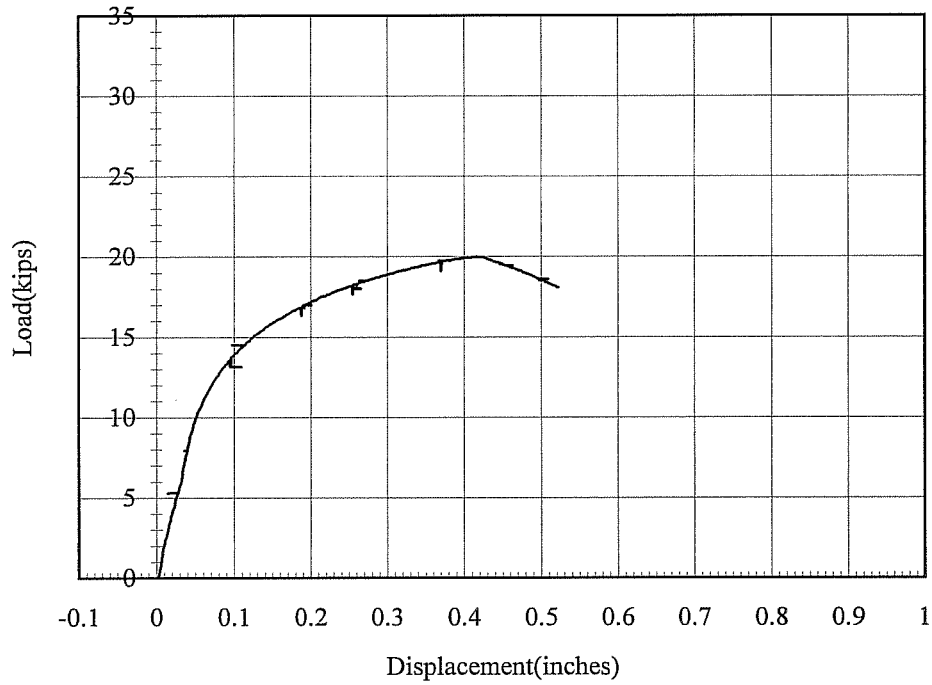

Figure B-1-1 AW300

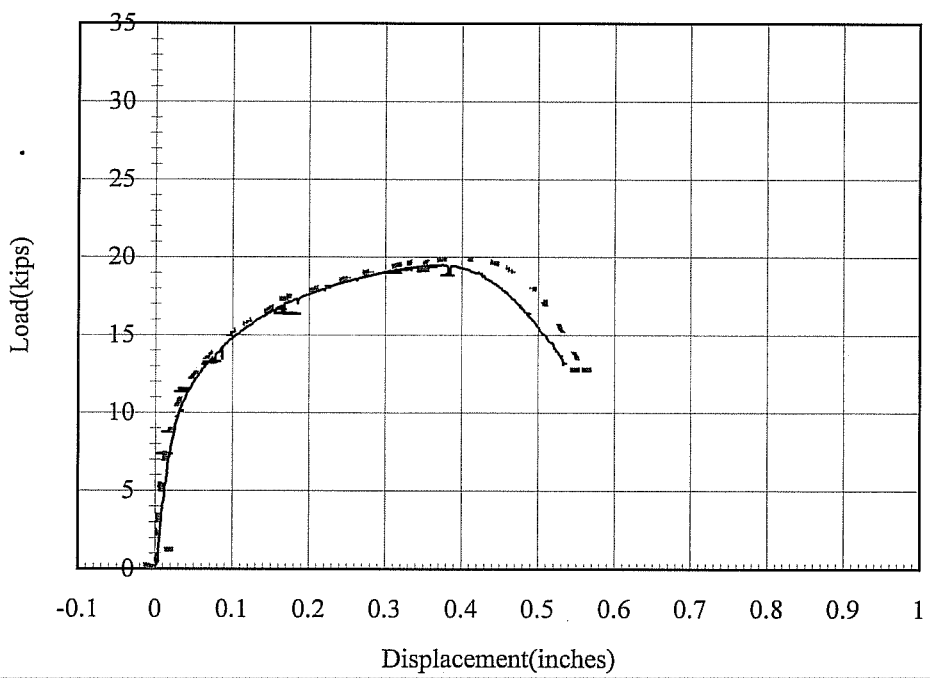

Figure B-1-2 AW350 and AW35R

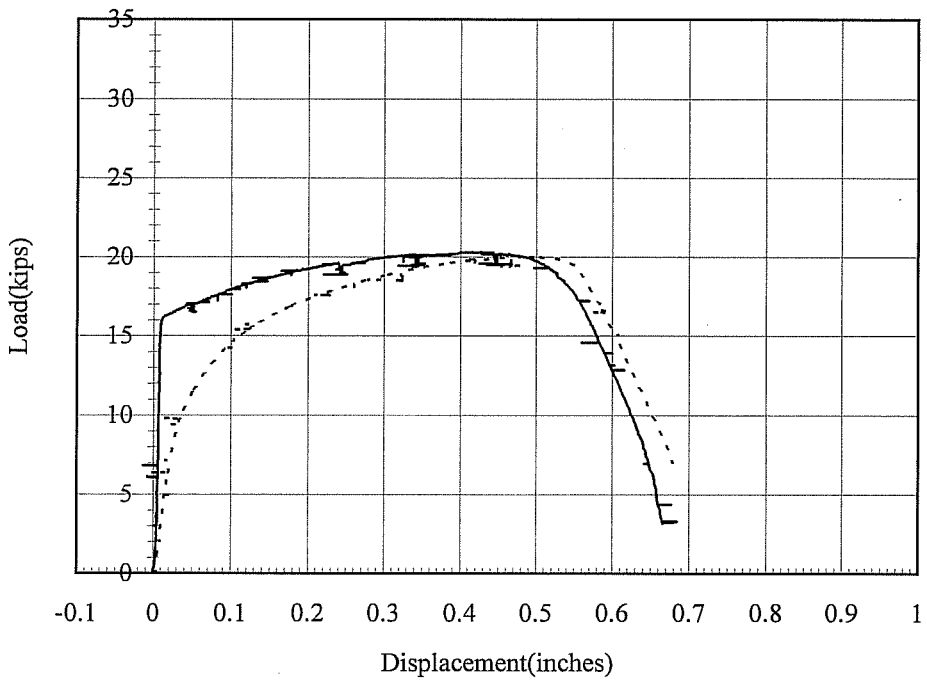

Figure B-1-3 AW45S and AW45U

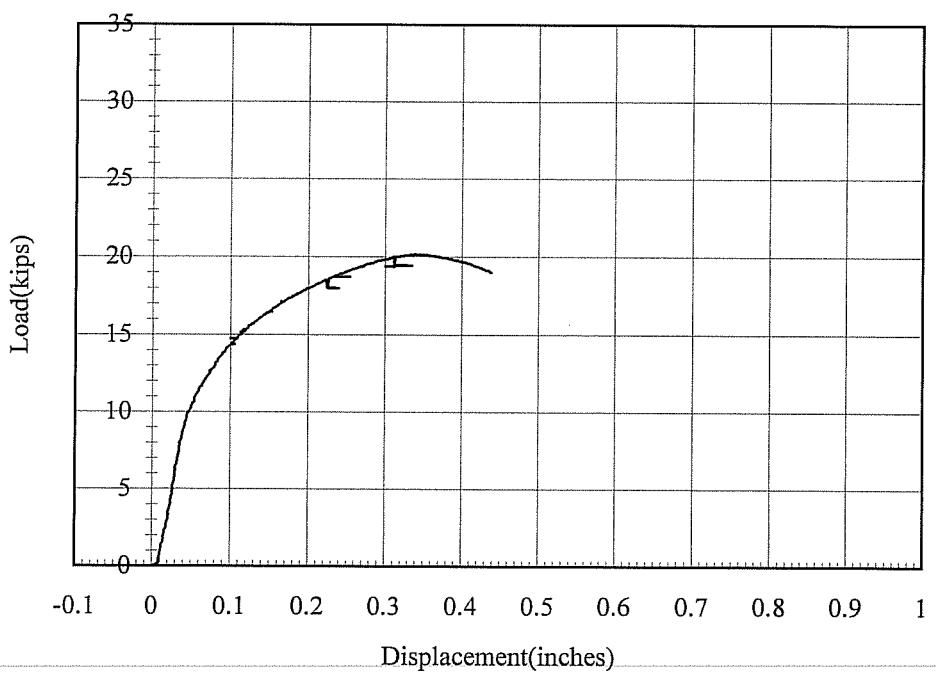

Figure B-1-4 AW600

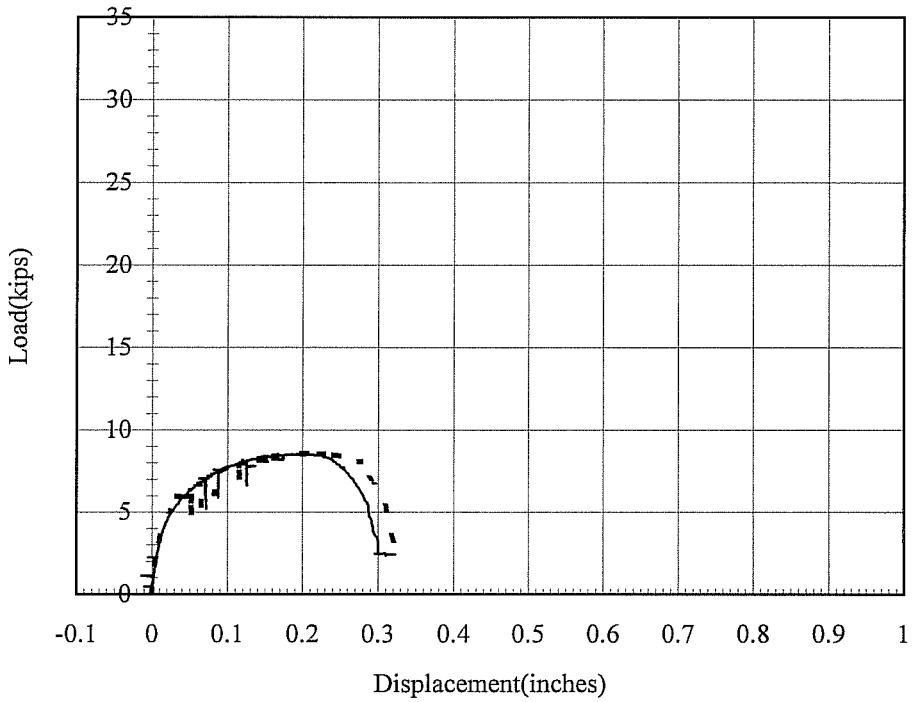

Figure B-2-1 AO050 and AO050R

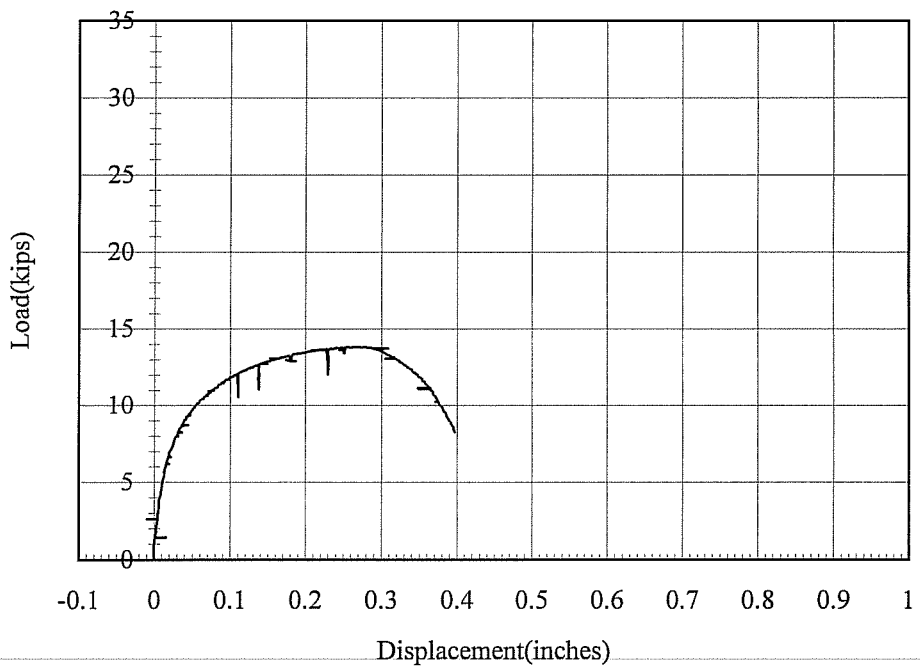

Figure B-2-2 AO100

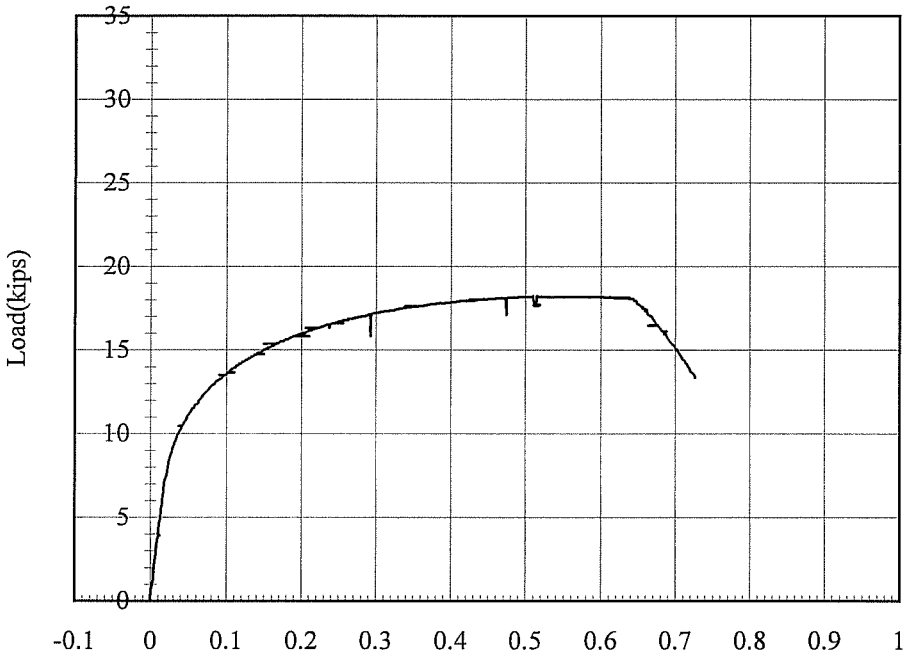

Figure B-2-3 AO150

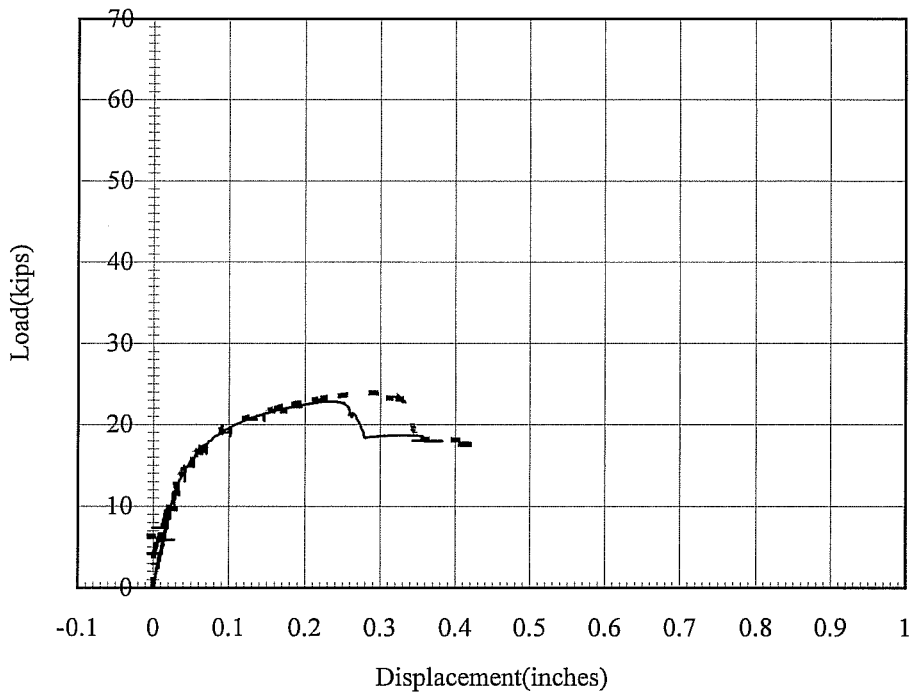

Figure B-3-1 AT0510 and AT0510R

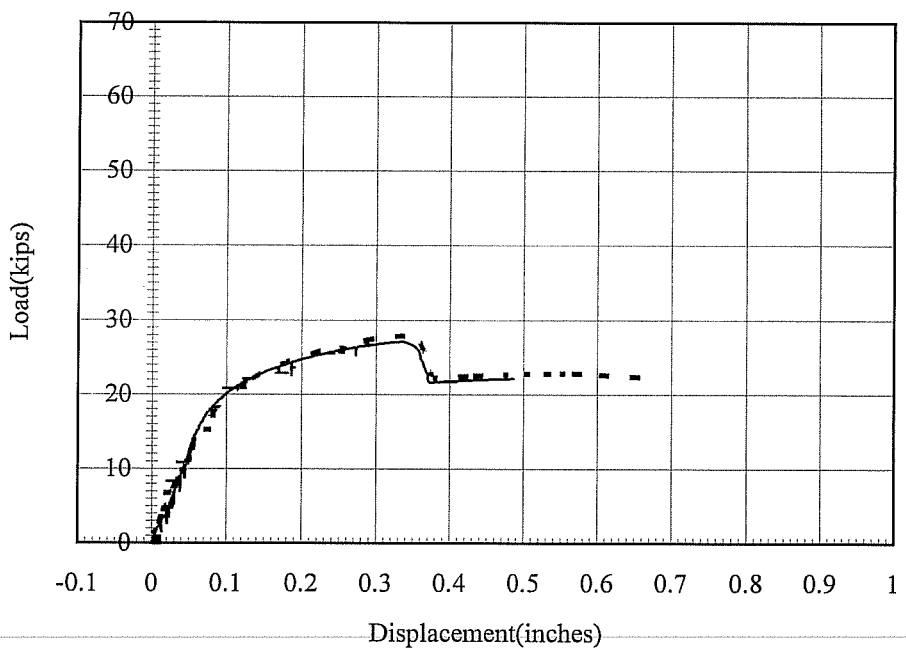

Figure B-3-2 AT0520 and AT0520R

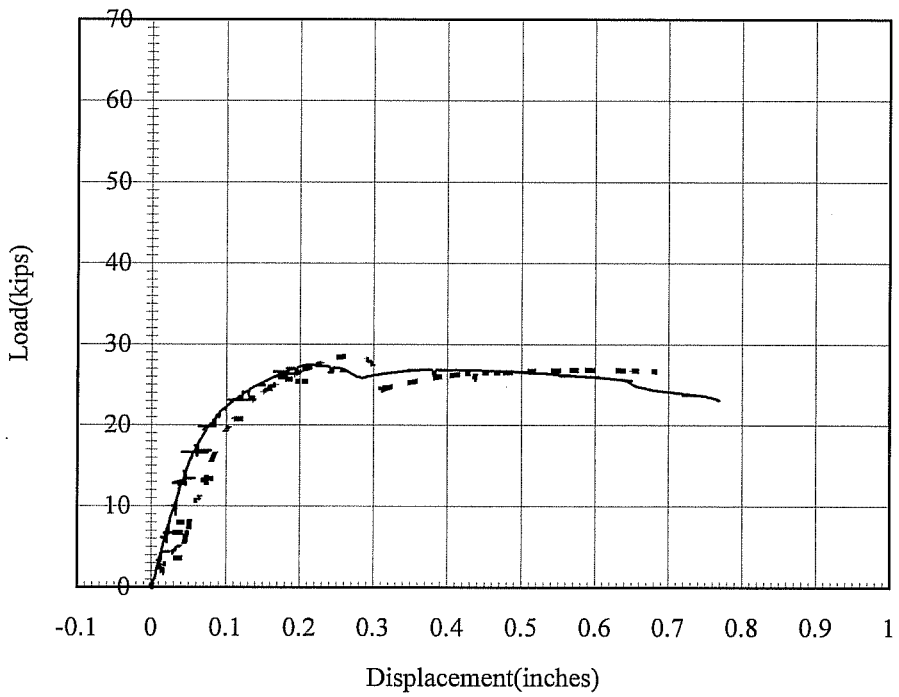

Figure B-3-3 AT0530 and AT0530R

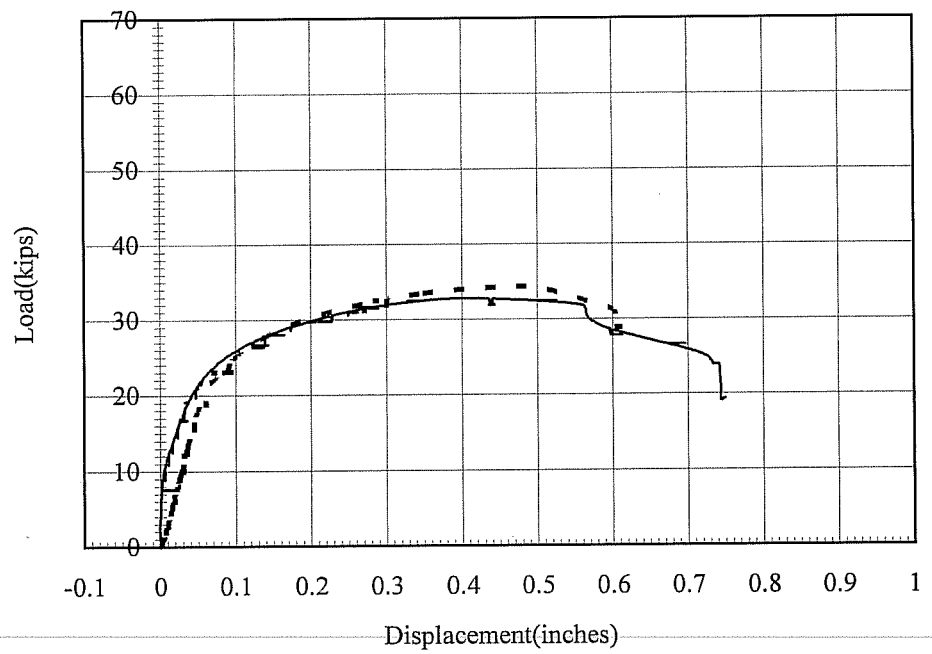

Figure B-3-4 AT1510 and AT1510R

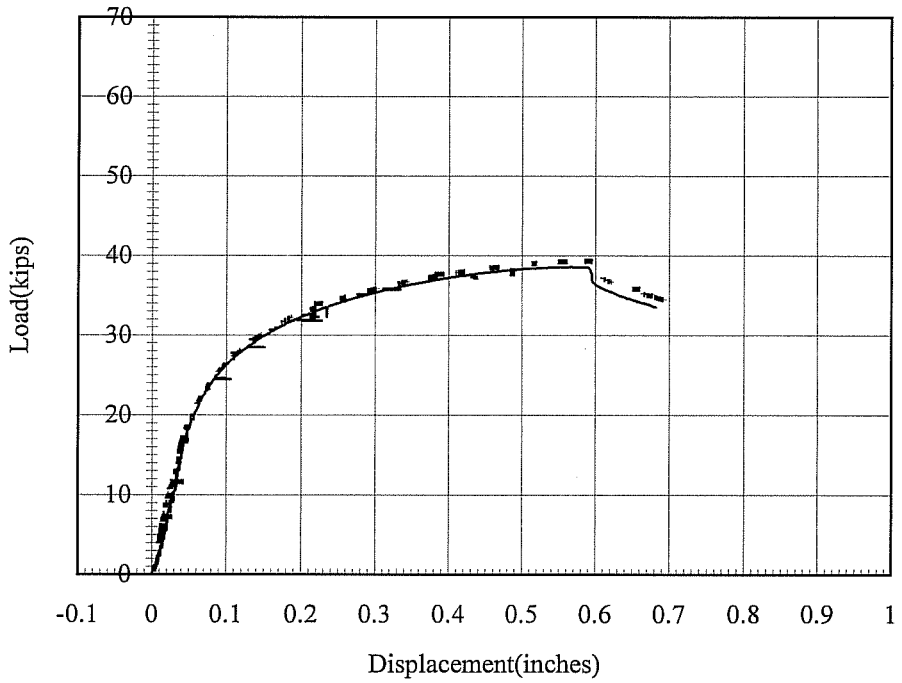

Figure B-3-5 AT1520 and AT1520R

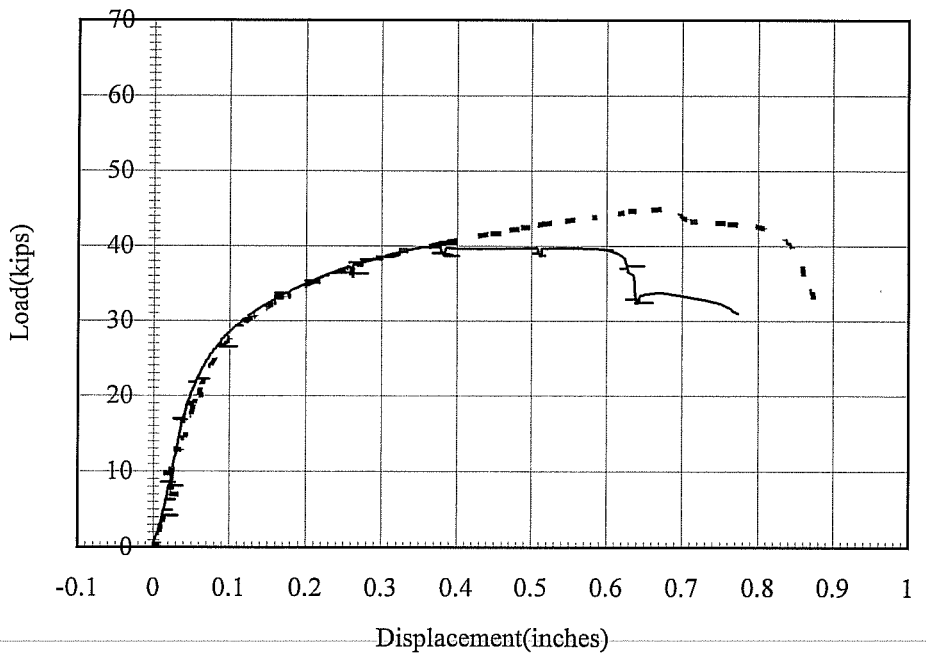

Figure B-3-6 AT1530 and AT1530R

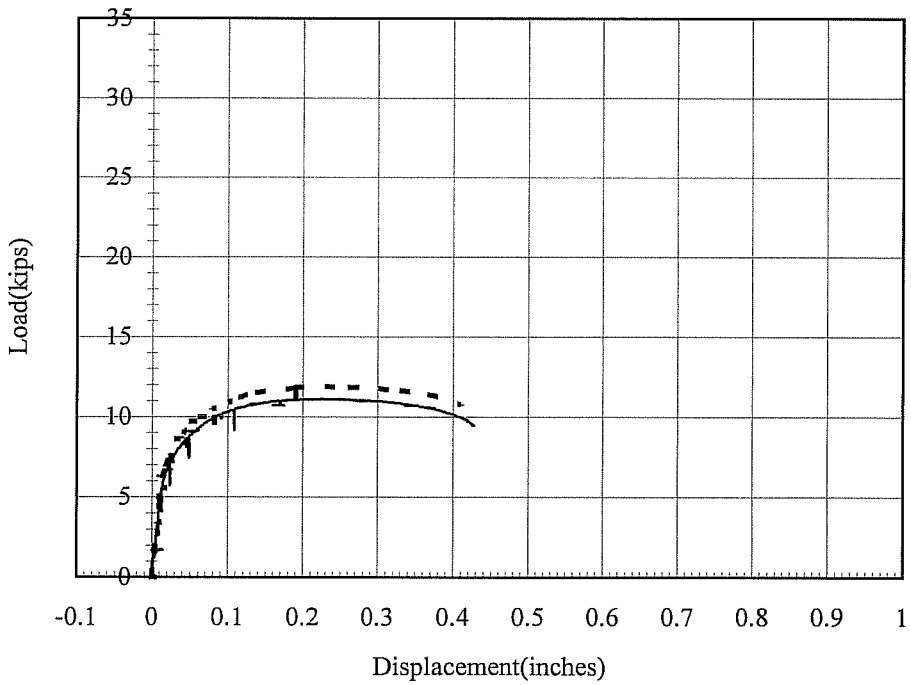

Figure B-4-1 BO050 and BO050R

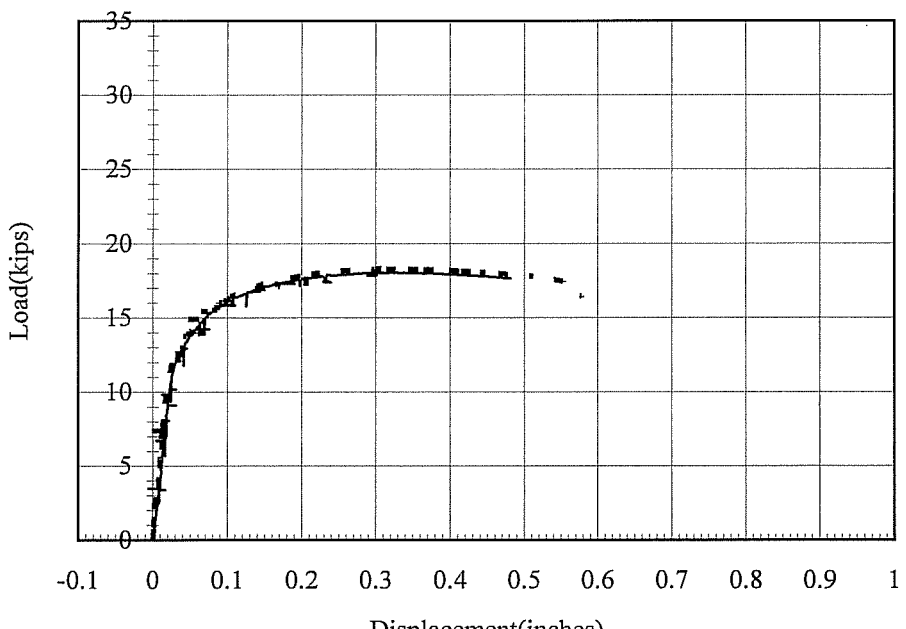

Figure B-4-2 BO100 and BO 100R

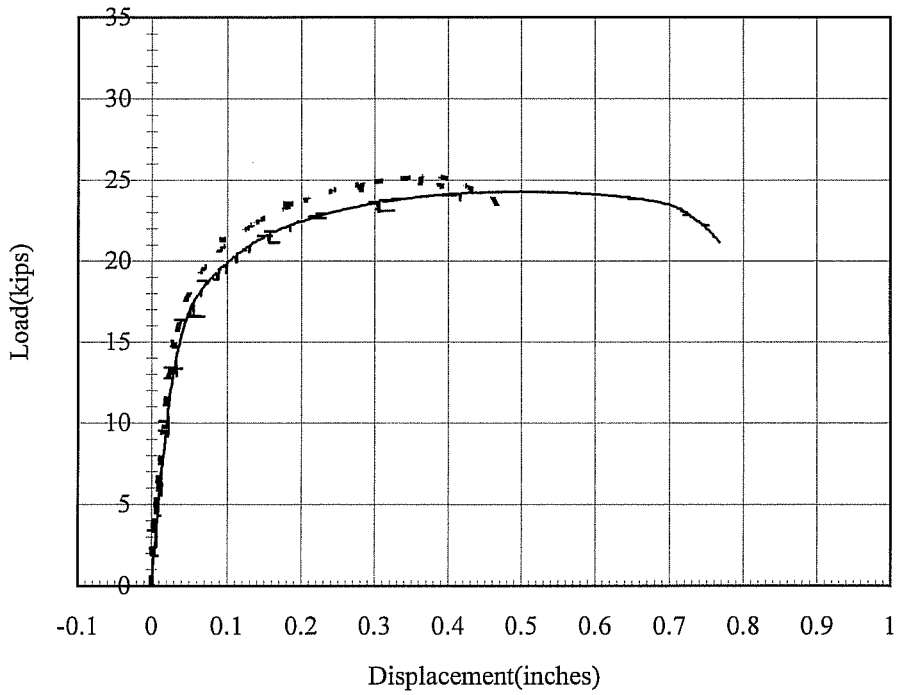

Figure B-4-3 BO150 and BO150R

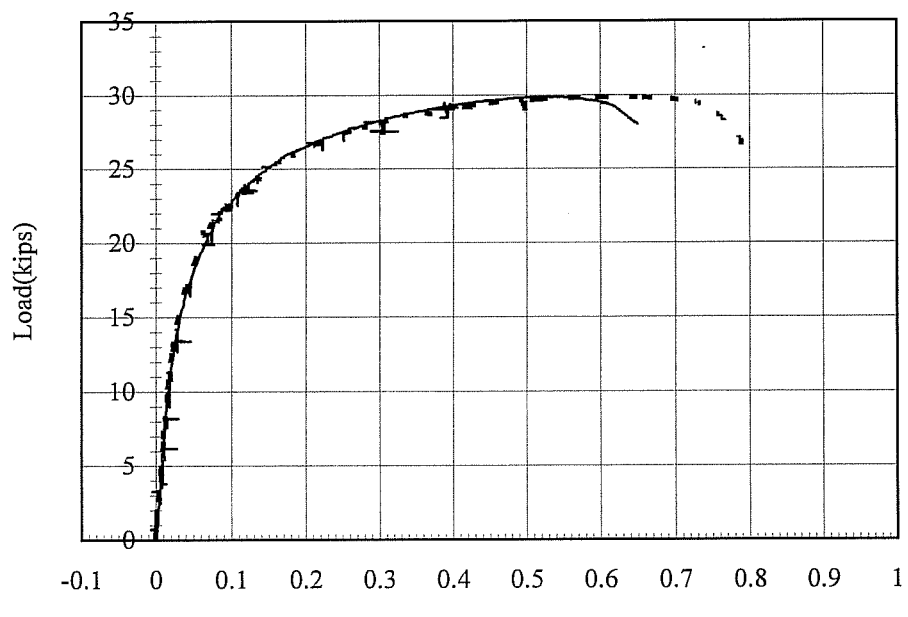

Figure B-4-4 BO200 and BO200R

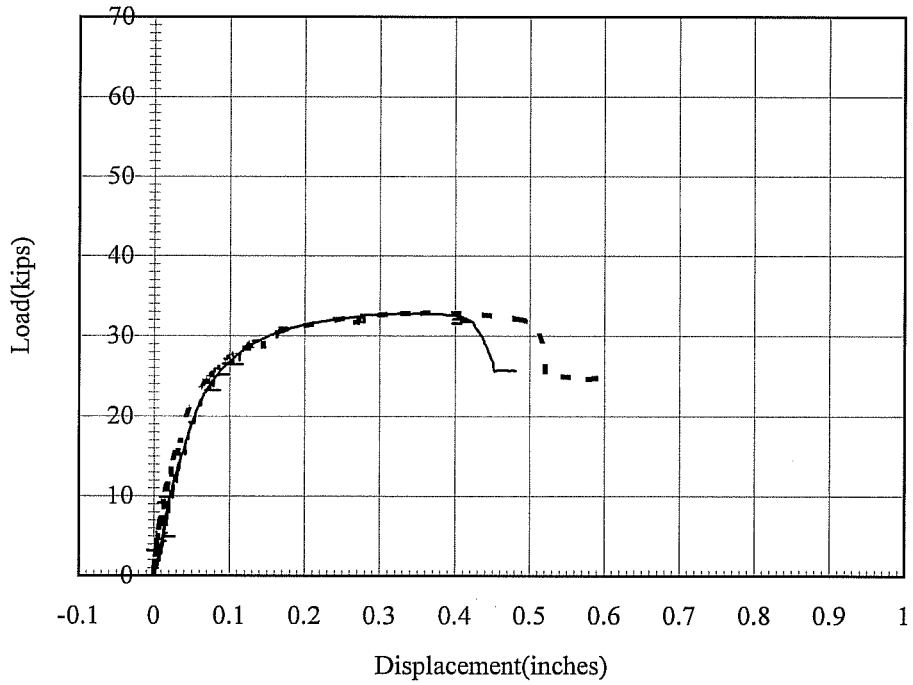

Figure B-5-1 BT0510 and BT0510R

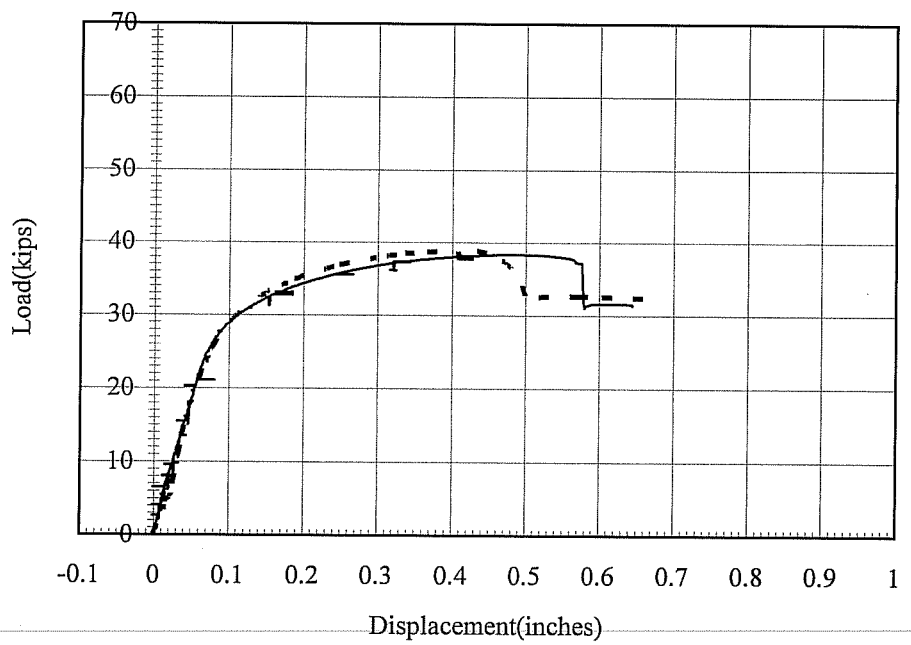

Figure B-5-2 BT0520 and BT0520R

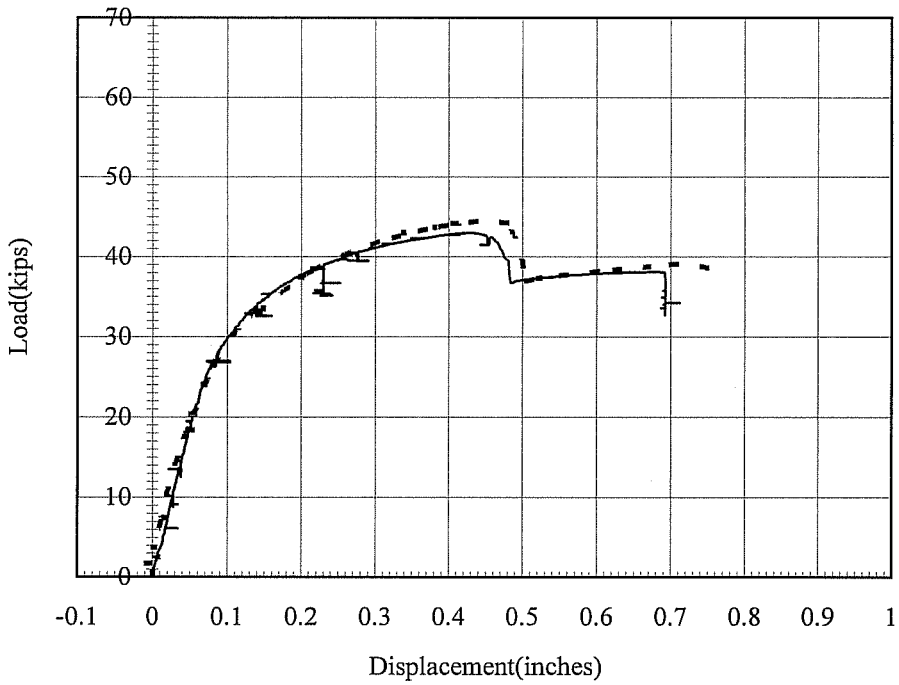

Figure B-5-3 BT0530 and BT0530R

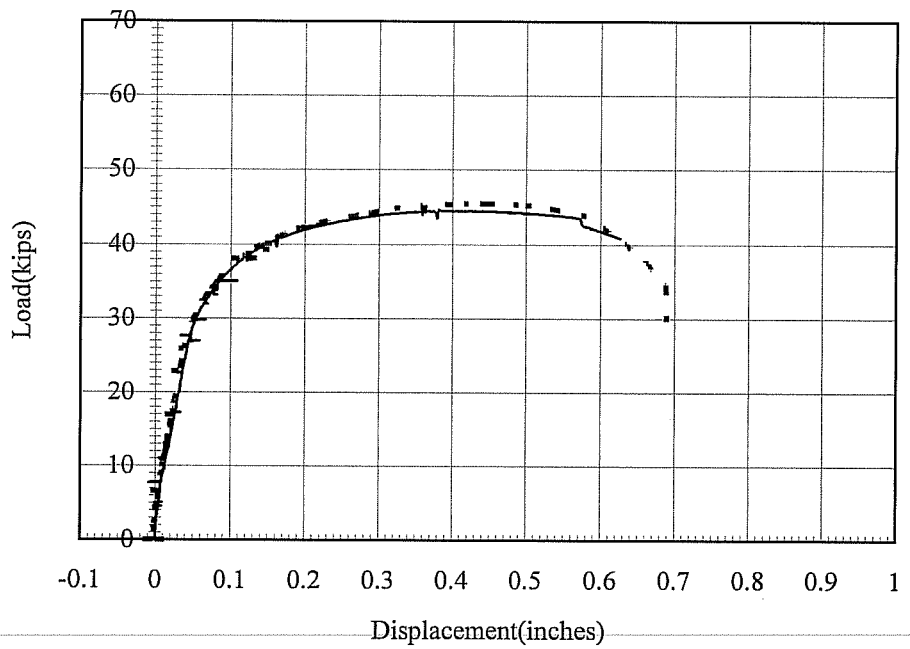

Figure B-5-4 BT1510 and BT1510R

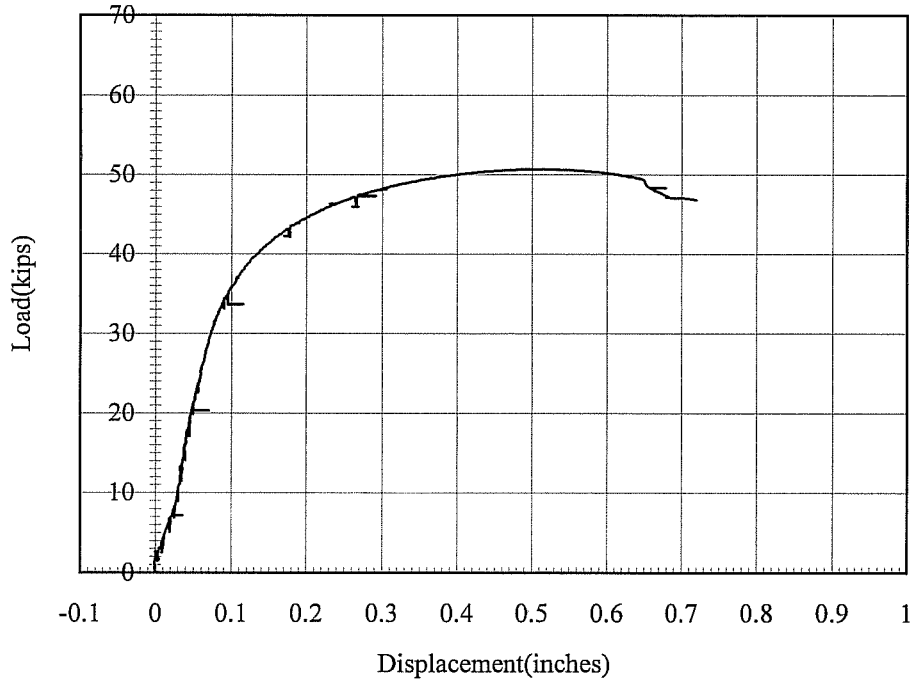

Figure B-5-5 BT1520

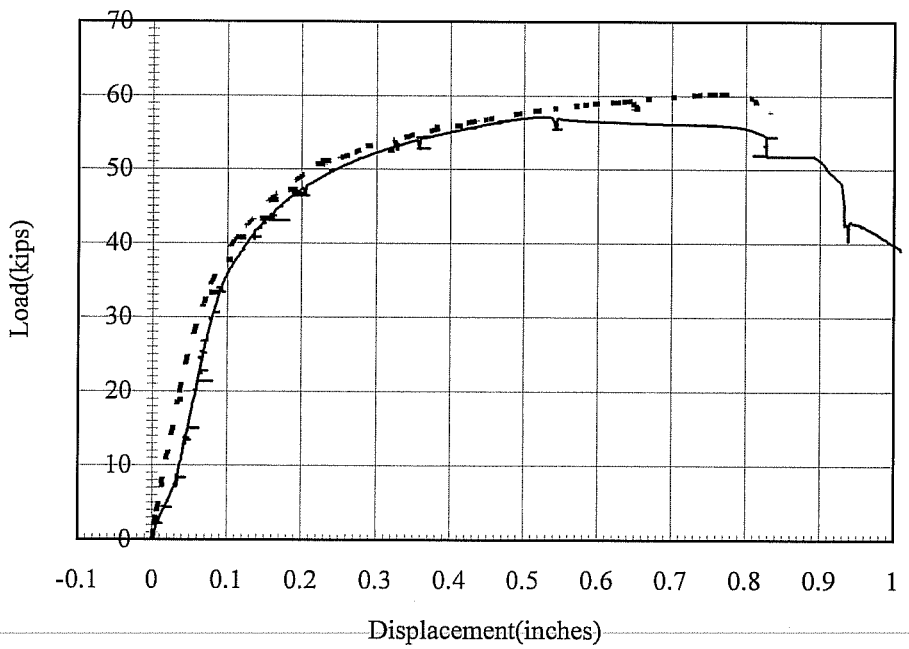

Figure B-5-6 BT1530 and BT1530R

LIST OF REFERENCES

1. American Institute of Steel Construction(1993), *Load and Resistance Factor Design Specifications for Structural Steel Buildings*, 2nd Ed., Chicago, IL.
2. American Institute of Steel Construction(1986), *Load and Resistance Factor Design Specifications for Structural Steel Buildings*, 1st Ed., Chicago, IL.
3. Chong, K.P. and Matlock, R.B.(1975), Light Gage Steel Bolted Connections without Washers, *Journal of the Structural Division*, ASCE, Vol. 101, No. ST7, July.
4. Frank, K.H. and Yura, J.A.(1981), An experimental Study of Bolted Shear Connections, *Report No. FWHA/RD-81/148*, Federal Highway Administration, U.S. Department of Transportation, Washington, D.C., December.
5. Gilchrist, R.T. and Chong, K.P.(1979), Thin Light Gage Bolted Connections without Washers, *Journal of the Structural Division*, ASCE, Vol. 105 , No. ST1, January.
6. Haussler, R.W. and Pabers, R.F.(1976), Discussion: Light-Gage Steel Bolted Connections without Washers, *Journal of Structural Division*, ASCE, Vol. 102, No. ST12, December, pp2375-2376.
7. Kennedy, J.B. and Sinclair G.R.(1969), Ultimate Capacity of Single Bolted Angle Connections, *Journal of the Structural Division*, ASCE, Vol. 95, No. ST8, August.
8. Kulak, G.L., Fisher, J.W., and Struik, J.H.A.(1987), *Guide to Design Criteria for Bolted and Riveted Joints*, 2nd Ed., A Wiley-Interscience publication, pp112-116, pp141-144.
9. Lewis, B.E.(1994), Edge Distance, Spacing, and Bearing in Bolted Connections, *Master of Science Report*, Oklahoma State University.
10. Perry, W.C.(1981), The Bearing Strength of Bolted Connections, *Master of Science Thesis*, The University of Texas at Austin, August.
11. Winter, M.(1956), Tests on Bolted Connections in Light Gage Steel, *Journal of the Structural Division*, ASCE, Proceedings of the American Society of Civil Engineers, Vol. 82, No. ST2, March.

12. Yura, J.A. and Frank, K.H.(1994), Proposal on the LRFD Formulation of Bearing Resistance in terms of Clear Dimensions, *Minutes of the June 3, 1994 meeting of the Research Council on Structural Connections*.
13. Ibrahim, F.S.(1995), Development of Design Procedures for Steel Girder Bolted Splices, *Doctor of Philosophy Dissertation*, The University of Texas at Austin, December

VITA

Hyeong Jun Kim was born in Seoul, Korea on September 15, 1971, to Moon-Sik Kim and Kyu-Hui Kim. After graduating from Cham-Sil High School in Seoul, Korea in 1990, he entered the Yonsei University in Seoul, Korea. The degree of Bachelor of Science was received in 1994. In August, 1994, he entered the Graduate School of the University of Texas at Austin.

Permanent Address: 3-901 Plaza Apt. Kil-dong
Seoul, Korea

This thesis was typed by the author.